Vernalization-triggered expression of the antisense transcript *COOLAIR* is mediated by *CBF* genes

Myeongjune Jeon[1†], Goowon Jeong[1†], Youbong Hyun[1,2], and Ilha Lee[1,2*]

[1]School of Biological Sciences, Seoul National University, Seoul 08826, Korea

[2]Research Center for Plant Plasticity, Seoul National University, Seoul 08826, Korea

[*]For correspondence: ilhalee@snu.ac.kr

[†]These authors contributed equally to this work

Abstract

Many plants undergo vernalization, a long-term winter-triggered acceleration of flowering, to align their flowering time with spring. In *Arabidopsis thaliana*, this is achieved by silencing a floral repressor, *FLOWERING LOCUS C* (*FLC*). *COOLAIR*, an antisense noncoding RNA expressed at the *FLC* locus, is induced during the early phase of vernalization, preceding *FLC* suppression. However, the mechanism by which long-term cold induces *COOLAIR* is not well understood. Here, we showed that C-repeat (CRT)/dehydration-responsive elements (DREs) at the 3′-end of *FLC* and CRT/DRE-binding factors (CBFs) are required for vernalization-induced *COOLAIR* activation. The CBFs bind to CRT/DREs at the 3′-end of *FLC,* both *in vitro* and *in vivo*, and the CBFs levels increased gradually during vernalization. Additionally, vernalization-induced *COOLAIR* expression was highly suppressed in the *cbfs* mutant, in which all *CBF*s were knocked-out. Contrastingly, *CBF*-overexpressing plants showed *COOLAIR* upregulation, even at warm temperatures. We propose that *COOLAIR* is induced by CBFs in the early phase of vernalization but is downregulated as CBFs are evicted from closed *FLC* chromatin during the late vernalization phase. We also demonstrated that *cbfs* and $FLC_{\Delta COOLAIR}$ mutants have a normal vernalization response, although they show defects in vernalization-induced *COOLAIR* activation, indicating that *COOLAIR* is not necessary for this process.

Introduction

Appropriate timing of flowering ensures plant reproductive success, which in turn provides evolutionary advantages. As sessile organisms, plants have evolved mechanisms by which reproductive growth is coordinated with seasonal cues. In many flowering plants, exposure to long-term winter cold is required for transition to the reproductive phase (*Chouard, 1960*). Vernalization, an acquisition of flowering competence in response to prolonged winter cold, allows plants to synchronize the timing of flowering with spring (*Chouard, 1960; Michaels and Amasino, 2000*).

Vernalization in *Arabidopsis thaliana* is mainly achieved by silencing a floral repressor gene, *FLOWERING LOCUS C* (*FLC*) (*Michaels and Amasino, 1999; Sheldon et al., 1999; Sheldon et al., 2000; Michaels and Amasino, 2001*). *FLC* encodes a MADS-box protein that directly associates with the promoter regions of floral activator genes, *SUPPRESSOR OF CO1* (*SOC1*) and *FLOWERING LOCUS T* (*FT*), which encodes florigen, and represses their expression (*Lee et al., 2000; Michaels et al., 2005; Helliwell et al., 2006*). *FLC* is highly expressed in winter annuals of Arabidopsis, such as San Feliu-2 and Lov-1, because of the strong transcriptional activation by the FRIGIDA (FRI) supercomplex which recruits general transcription factors, as well as several chromatin modifiers (*Michaels and Amasino, 1999; Sheldon et al., 1999; Johanson et al., 2000; Choi et al., 2011; Li et al., 2018*). Therefore, winter annuals show a late-flowering phenotype, but their flowering is dramatically accelerated by vernalization-induced *FLC* silencing (*Napp-Zinn, 1955; Lee et al., 1993; Clarke and Dean, 1994; Koornneef et al., 1994; Lee et al., 1994*). In contrast to winter annuals, rapid-cycling accessions, such as Columbia (Col) and Landsberg *erecta* (L*er*), exhibit early flowering due to mutations in *FRI* and/or *FLC* (*Johanson et al., 2000; Gazzani et al., 2003; Michaels et al., 2003*). However, the autonomous pathway (AP) mutants in Col and L*er* background also show late flowering with an increased level of *FLC*; vernalization causes the epigenetic suppression of *FLC*, thus accelerating their flowering to a degree similar to that seen in winter annuals (*Koornneef et al., 1998; Michaels and Amasino, 2001*).

In Arabidopsis winter annuals, flowering is prevented by strong expression of *FLC* during fall. Consistently, *FLC* chromatin is highly enriched with active histone marks such as histone

55 H3 acetylation and trimethylation of Lys4 or Lys36 at H3 (H3K4me3/H3K36me3) (*Bastow et*
56 *al., 2004; Yang et al., 2014*). During winter, *FLC* chromatin is gradually deacetylated, and the
57 H3K4me3 and H3K36me3 on *FLC* are removed concomitantly (*Bastow et al., 2004; Yang et*
58 *al., 2014*). Additionally, the repressive histone marks, H3 Lys9 dimethylation (H3K9me2) and
59 H3 Lys27 trimethylation (H3K27me3), are accumulated by the polycomb repressive complex
60 2 (PRC2) in the nucleation region around the first exon and intron of *FLC* (*Sung and Amasino,*
61 *2004; Wood et al., 2006; De Lucia et al., 2008; Angel et al., 2011*). Subsequently in the
62 following spring, H3K27me3 is spread to the entire *FLC* chromatin region by LIKE
63 HETEROCHROMATIN PROTEIN 1, which ensures stable *FLC* suppression and renders
64 plants competent to flower (*Mylne et al., 2006; Yang et al., 2017*).

65 Several long-term cold-induced factors have been shown to play a crucial role in the
66 epigenetic silencing of *FLC*. *VERNALIZATION INSENSITIVE 3* (*VIN3*) family genes, which
67 are upregulated by prolonged cold, encode PHD (Plant Homeodomain)-finger domain proteins
68 which recognize H3K9me2 enriched in the *FLC* chromatin during the vernalization process
69 (*Sung and Amasino, 2004; Kim and Sung, 2013*, *2017a*). These proteins mediate the
70 recruitment of PRC2 and subsequent deposition of H3K27me3 at the nucleation region of *FLC*
71 (*Sung and Amasino, 2004; De Lucia et al., 2008; Kim and Sung, 2013*). In addition,
72 vernalization-induced long noncoding RNAs (lncRNAs) are involved in such histone
73 modifications. *COLDAIR* and *COLDWRAP*, the two lncRNAs transcribed from the first intron
74 and promoter region of *FLC*, respectively, are necessary for H3K27me3 deposition in response
75 to long-term cold (*Heo and Sung, 2011; Kim and Sung, 2017b*). Additionally, *COLDAIR* and
76 *COLDWRAP* are thought to affect the formation of the intragenic chromatin loop at *FLC*, which
77 may be part of the *FLC* silencing mechanism (*Kim and Sung, 2017b*).

78 Unlike *COLDAIR* and *COLDWRAP,* which are transcribed in the sense direction of *FLC*,
79 *COOLAIR* is an antisense transcript expressed from the 3′-end of *FLC* (*Swiezewski et al., 2009*).
80 The gradual accumulation of *COOLAIR* reaches a maximum within a few weeks of winter cold,
81 whereas the other lncRNAs, *COLDAIR* and *COLDWRAP*, show peaks at a later phase of
82 vernalization (*Csorba et al., 2014; Kim and Sung, 2017b*). Since the *COOLAIR* promoter is
83 sufficient to confer cold-induced silencing of a reporter gene when added to the 3′-region of

the gene (*Swiezewski et al., 2009*), extensive efforts have been made to elucidate how *COOLAIR* antagonizes *FLC* expression. One possibility is that *COOLAIR* facilitates changes in the chromatin environment of *FLC*. *COOLAIR* has been reported to be involved in removing active histone marks, H3K4 and H3K36 methylations from *FLC* chromatin, thus leading to *FLC* suppression (*Helliwell et al., 2011; Csorba et al., 2014; Berry and Dean, 2015*). Co-transcriptional events governed by *COOLAIR*-targeted RNA-processing factors, including some factors involved in the autonomous pathway for flowering, seem to be critical for switching the *FLC* chromatin state (*Wu et al., 2020*). Furthermore, *COOLAIR* is also likely necessary for H3K27me3 deposition via interaction with FLOWERING CONTROL LOCUS A (FCA) protein (*Tian et al., 2019*).

Compared to the functional mechanism of *COOLAIR* in *FLC* silencing, how long-term cold triggers *COOLAIR* induction is less well-understood. Previous studies have inferred that the regulatory region conferring long-term cold response of *COOLAIR* is well-conserved among relatives of Arabidopsis (*Swiezewski et al., 2009; Castaings et al., 2014; Csorba et al., 2014; Berry and Dean, 2015*). However, little is known about their upstream regulators. Although a recent report has shown that an NAC domain-containing protein, NTM1-LIKE 8 (NTL8), can bind to the *COOLAIR* promoter and activate its expression, it has not been thoroughly addressed whether NTL8 is necessary for vernalization-induced *COOLAIR* activation (*Zhao et al., 2021*). In the present study, we identified that CRT/DREs at the 3′-end of *FLC* are required for the long-term cold response of *COOLAIR*. Additionally, we showed that CRT/DRE-binding factors (CBFs), which accumulate through the long-term winter cold, act as upstream regulators of *COOLAIR* during vernalization.

Results

A CRT/DRE-binding factor, CBF3, directly binds to CRT/DREs at the 3′-end of *FLC*

Since it has already been shown that the proximal promoter region of *COOLAIR* is highly conserved among the *FLC* orthologs from *A. thaliana* relatives (*Castaings et al., 2014*), we assumed that the *cis*-element conferring long-term cold response would exist within that region. A comparison of the region near the transcriptional start site of *COOLAIR* revealed that two CRT/DREs are well-conserved among six *FLC* orthologs from five related species in the Brassicaceae family (*Figure 1A*). CRT/DRE, whose core sequence is CCGAC, is a regulatory element that imparts cold- or drought-responsive gene expression (*Baker et al., 1994*). Three *CBF* family genes, *CBF1*, *2*, and *3*, have been known to encode AP2 (APETALA2) domain-containing proteins that can bind to CRT/DRE, and are usually present in the promoters of cold- and drought-regulated genes (*Stockinger et al., 1997; Medina et al., 1999*). Consistent with this, the Arabidopsis cistrome database suggests that the CBFs bind to the 3′-end sequence of *FLC* containing CRT/DREs (*Figure 1—figure supplement 1; O'Malley et al., 2016*).

To confirm this binding, we performed electrophoretic mobility shift assay (EMSA) using probes harboring the CRT/DREs (DRE1 or -2) from the *COOLAIR* promoter. The mobility of these two Cy5-labelled probes was retarded by maltose-binding protein (MBP)-fused CBF3 (*Figure 1B, Figure 1-figure supplement 2*). The band shift was competed out by adding an excess amount of non-labelled DRE1 or 2 oligonucleotides (*Figure 1B, Figure 1—figure supplement 2*). By contrast, the competitors containing the mutant forms of DRE1 or 2 ($DRE1^m$ or 2^m respectively) failed to compete (*Figure 1B*). We also tested the binding of other CRT/DRE-like sequences distributed in the *FLC* locus. Two of these (DREa and b) were present in the *FLC* promoter, while the other two, DREc and d, were present in the first and last exons, respectively (*Figure 1—figure supplement 2*). Among these, only DREc competed with the band shift caused by the CBF3-DRE1 interaction (*Figure 1B*).

Subsequently, a chromatin immunoprecipitation (ChIP) assay using a *CBF3*-overexpressing transgenic plant, *pSuper::CBF3-myc* (*Liu et al., 2017*), was performed to determine whether CBF3 is associated with the region of *FLC* containing CRT/DREs *in vivo*. Consistent with the *in vitro* results, the CBF3-myc protein was enriched at the 3′-end of *FLC*

135 as well as the first exon of *FLC*, where DREc was located (*Figure 1C*). Without vernalization
136 (NV), CBF3-myc was highly enriched at both the 5′- and 3′-ends of *FLC* (P1 and P3), indicating
137 that CBF3 protein can activate *FLC* in warm conditions, as previously reported (*Seo et al.,*
138 *2009*). However, the enrichment on the P1 region rapidly disappeared during the vernalization
139 period. By contrast, the enrichment on P3 was maintained until 10 days of vernalization (10V)
140 and was subsequently reduced (*Figure 1C*). This is coincident with the expression pattern of
141 *COOLAIR*, which declines in the late phase of vernalization (*Csorba et al., 2014*).

142

143 ***COOLAIR* is one of the CBF regulons in Arabidopsis**

144 *CBF* genes are rapidly and transiently induced upon exposure to cold (*Medina et al., 1999*).
145 CBF regulons, which are CBF-targeted genes, are correspondingly up- or down-regulated after
146 a few hours-long cold interval (*Gilmour et al., 1998; Liu et al., 1998; Fowler and Thomashow,*
147 *2002*). As *COOLAIR* bears CBF3-binding sites in its promoter (*Figure 1*), it was expected that
148 *COOLAIR* would show CBF regulon-like expression.

149 The expression of genes assigned to the CBF regulon is up- or downregulated by *CBF*
150 overexpression under warm condition (*Park et al., 2015*). Likewise, we found that the total
151 transcript level of *COOLAIR* increased in *CBF3*-overexpressing transgenic plants
152 (*pSuper::CBF3-myc*) grown at room temperature (22°C), as compared to that in the wild-type
153 (Col-0) (*Figure 2A*). Such upregulation was mainly due to type I or type IIi *COOLAIR* isoforms.
154 As the levels of both proximal (type I) and distal (type II) isoforms of *COOLAIR* were higher
155 in the *CBF3* overexpressor than in the wild-type, it is likely that *COOLAIR* transcription,
156 instead of the 3′-processing event, is affected by CBF3 (*Figure 2A; Liu et al., 2010; Marquardt*
157 *et al., 2014*). It has been reported that the targets of CBF1 or -2 are not entirely identical to
158 those of CBF3, although *CBF* genes show high sequence similarity (*Novillo et al., 2007*). Thus,
159 we compared the expression levels of all *COOLAIR* isoforms in transgenic plants
160 overexpressing *CBF1, -2,* and *-3* (*Seo et al., 2009*). Overall, all *CBF*-overexpressing plants
161 showed increased levels of *COOLAIR* (*Figure 2—figure supplement 1*). However, each *CBF*-
162 overexpressing plant showed a subtly different effect on *COOLAIR* expression. The *CBF2*
163 overexpressor showed the highest level of the proximal *COOLAIR* isoform, whereas the *CBF3*

overexpressor showed the highest level of distal *COOLAIR*. By contrast, the *CBF1*-overexpressing plants showed a slightly smaller increase of proximal *COOLAIR* levels and a negligible increase in distal *COOLAIR,* as compared to those in the wild-type, Ws-2. Such results imply that the three CBFs regulate *COOLAIR* transcription subtly differently.

Another characteristic of CBF regulons is that they are induced by a day of cold exposure (*Park et al., 2015*). Thus, we checked if *COOLAIR* is also induced by short-term cold. Wild-type (*FRI* Col) plants were treated with 0, 0.5, 1, 1.5, 2, 3, 6, and 24 h of cold (4°C), then the levels of total *COOLAIR* were measured. The results showed that cold treatment less than 3 h failed to induce *COOLAIR* expression, although the *CBF*s expression reached a peak at 3 h of cold treatment (*Figures 2B and 3A; Gilmour et al., 1998*). Following 6 h of cold treatment, *COOLAIR* was conspicuously induced (*Figure 2B*). Thus, short-term cold induced *COOLAIR* expression similar to those of other CBF-targeted genes, *i.e.* the expression is highly increased after *CBF* levels reach a peak upon cold exposure (*Fowler and Thomashow, 2002*). To confirm whether *CBF*s are responsible for the rapid cold response of *COOLAIR*, we checked *COOLAIR* induction in the wild-type and *cbfs-1* mutant, in which all three *CBF*s are knocked-out (*Jia et al., 2016*), after a day of cold treatment (*Figure 2C*). All isoforms, as well as total *COOLAIR*, failed to be induced by short-term cold exposure in the *cbfs* mutant, although a drastic increase was observed in the wild-type. Thus, the results strongly suggested that *CBF*s are required for *COOLAIR* induction, even under a short period of cold exposure.

CBFs accumulate during vernalization

We subsequently questioned whether *CBF*s are also responsible for the induction of *COOLAIR* during vernalization. *COOLAIR* is gradually upregulated as the cold period persists and peaks after 2-3 weeks of vernalization (*Csorba et al., 2014*). However, most studies on *CBF* expression have been performed within a few days, since the function of *CBF*s has been analyzed only in the context of short-term cold (*Gilmour et al., 1998; Liu et al., 1998; Medina et al., 1999; McKhann et al., 2008*). Therefore, we investigated the expression patterns of *CBF*s before and after long-term cold exposure, to find a correlation between the expression of *CBF*s and *COOLAIR* during vernalization. As previously shown, the levels of all three *CBF*s reached

193 their peaks within 3 h of cold exposure, thereafter decreased rapidly (*Figure 3A*). However, the
194 expression of *CBF*s increased again as the cold period was prolonged (>20V), suggesting that
195 both short-term and vernalizing cold treatments upregulated *CBF* expression (*Figure 3B*).

196 Since *CBF*s are known to be regulated by circadian rhythms (*Dong et al., 2011*), we also
197 investigated whether the circadian rhythm affects vernalization-induced *CBF* expression. For
198 this, we collected wild-type (Col-0) plants every 4 h under a short-day cycle (SD, 8 h light/16
199 h dark), in both the NV and 40V conditions. As shown in *Figure 3C*, although the rhythmic
200 pattern of each *CBF* was variable, the overall transcript levels of all three *CBF*s were much
201 higher at 40V than at NV.

202 To verify whether the increased transcription of *CBF3* led to protein accumulation, we
203 also measured the level of CBF3 at each time-point of vernalization using the *pCBF3::CBF3-*
204 *myc* plant (*Jia et al., 2016*). In accordance with the rapid and transient induction of *CBF3* under
205 short-term cold (*Medina et al., 1999*), CBF3 was highly expressed after a day of cold exposure
206 (1V), but decreased at 10V (*Figure 3D*). However, as the period of cold exposure was
207 prolonged, the CBF3 level was re-increased such that the level at 40V was similar to that at 1V.
208 The increased protein level after 40V rapidly decreased if the plants were transferred to room
209 temperature for 4 d (40VT4). Such results suggested that CBFs are responsible for the
210 progressive upregulation of *COOLAIR*, at least during the early phase of vernalization (*Csorba*
211 *et al., 2014*).

212

213 ***CBF*s are involved in vernalization-induced *COOLAIR* expression**

214 To clarify whether *CBF*s are responsible for long-term cold-mediated *COOLAIR* induction, we
215 quantified *COOLAIR* levels in the wild-type and *cbfs* mutant during the vernalization process.
216 Although the level of total *COOLAIR* gradually increased until 20V, and then decreased
217 afterward in the wild-type as previously reported (*Csorba et al., 2014*), the level in *cbfs* mutant
218 was severely reduced across the entire vernalization period (*Figure 4A*). It suggests that *CBF*s
219 are required for full induction of *COOLAIR* in the early phase of vernalization.

220 Consistent with the suppressed *COOLAIR* expression in *cbfs* mutants, the *CBF3*

221 overexpressor, *pSuper::CBF3-myc,* showed a much higher *COOLAIR* level than the wild-type
222 (Col-0), throughout the vernalization period (*Figure 4B*). It is noteworthy that *COOLAIR*
223 expression in *pSuper::CBF3-myc* was further upregulated by cold, especially during the early
224 vernalization phase (10V) (*Figure 4B*). This result implies that both transcriptional and post-
225 transcriptional regulation of CBFs are involved in the long-term cold response of *COOLAIR*.

226 A recent study has shown that the first seasonal frost (<0°C) during the winter season
227 strongly induces *COOLAIR* expression (*Zhao et al., 2021*). Therefore, we tested whether *CBF*s
228 are also required for the strong induction of *COOLAIR* triggered by freezing temperatures.
229 Wild-type and *cbfs* mutants were subjected to 20V, with or without an additional 8 h of -1°C
230 freezing treatment (8hF). In both the genotypes, the *COOLAIR* levels were increased upon 8hF
231 treatment, but *cbfs* mutants showed a much smaller increase compared to the wild-type (*Figure*
232 *4C*). Thus, *CBFs* seem to be responsible for both the gradual increase of *COOLAIR* during
233 vernalization and the strong *COOLAIR* induction triggered by freezing temperatures.

234

235 **CRT/DREs at the 3′-end of *FLC* are necessary for CBFs-mediated induction of *COOLAIR***
236 **during vernalization.**

237 Since CBF3 was able to bind to CRT/DREs in the first exon (DREc) and the 3′-end of *FLC*
238 (DRE1 and 2) (*Figure 1B-C*), we questioned whether CRT/DRE is responsible for the CBF-
239 mediated long-term cold response of *COOLAIR*. To address this, we performed an *A. thaliana*
240 protoplast transfection assay using the *35S::CBF3-HA* effector construct and
241 *pCOOLAIR*$_{DRE}$*::LUC* reporter construct, in which the 1 kb wild-type *COOLAIR* promoter was
242 fused to the luciferase reporter gene. The luciferase activity assay suggested that the CBF3-HA
243 protein activates transcription of the *COOLAIR* promoter (*Figure 5A*). By contrast, CBF3-HA
244 failed to increase luciferase activity when the mutant version of the *COOLAIR* promoter with
245 mutant DRE1 and 2 (*pCOOLAIR*$_{DRE}^{m}$*::LUC*) was used as a reporter (*Figure 5A*). Additionally,
246 co-transfection of the *35S::CBF3-HA* effector and *pFLC::LUC* reporter construct, which
247 harbors the 1 kb sequence including the promoter and first exon of *FLC*, did not show increased
248 luciferase activity (*Figure 5A*). These results strongly indicated that CBF3 can activate
249 *COOLAIR* transcription through DRE1 and 2 located in the promoter, but not via the first exon

250 of *FLC*.

251 To further determine whether the 3′-end region of *FLC* is required for the vernalization
252 response of *COOLAIR*, we measured *COOLAIR* expression in the wild-type and $FLC_{\Delta COOLAIR}$
253 mutant, which lacks a 324 bp portion of the *COOLAIR* promoter region (*Luo et al., 2019*),
254 before and after vernalization. Although the common *COOLAIR* transcriptional start site was
255 eliminated in $FLC_{\Delta COOLAIR}$, the proximal *COOLAIR* isoform (type I) was still detected,
256 probably due to alternative transcription start sites (*Figure 5B; Zhao et al., 2021*). As expected,
257 the expression of the proximal *COOLAIR* variant in the $FLC_{\Delta COOLAIR}$ mutant was not induced
258 at 20V, while the wild-type showed increased type I *COOLAIR* level at 20V (*Figure 5B*). Thus,
259 the *COOLAIR* promoter region containing two CRT/DREs is necessary for the long-term cold
260 response of *COOLAIR*.
261

262 **CBFs-mediated *COOLAIR* induction by vernalization is not necessary for *FLC* silencing**

263 Lastly, we investigated the role of *COOLAIR* induced by CBFs in the vernalization-triggered
264 *FLC* silencing process. *COOLAIR* is reported to facilitate the removal of H3K4me3 and
265 H3K36me3 from *FLC* chromatin during vernalization, whereas the other lncRNAs, *COLDAIR*
266 and *COLDWRAP*, are required for H3K27me3 deposition (*Csorba et al., 2014; Berry and Dean,*
267 *2015; Kim and Sung, 2017b*). Therefore, we compared the enrichment of H3K4me3,
268 H3K36me3, and H3K27me3 on *FLC* chromatin in non-vernalized or vernalized wild-type and
269 *cbfs* mutants. As reported (*Bastow et al., 2004; Sung and Amasino, 2004; Yang et al., 2014*),
270 there was a reduction in the enrichment of H3K4me3 and H3K36me3, whereas that of
271 H3K27me3 increased considerably in the nucleation region of *FLC* by 40V in the wild-type
272 (*Figure 6A-D*). Interestingly, although *COOLAIR* levels were significantly reduced in the *cbfs*
273 mutant (*Figure 4A*), vernalization-caused reductions in H3K4me3 and H3K36me3 levels and
274 increase in H3K27me3 levels were comparable to those in the wild-type (*Figure 6A-D*). This
275 result indicates that CBF-mediated *COOLAIR* induction is not necessary for vernalization-
276 induced epigenetic changes in *FLC* chromatin.

277 Consistent with the epigenetic changes in *FLC* chromatin in the *cbfs* mutant, the *FLC* level

was gradually suppressed during the vernalization process, and the suppression was maintained after 40VT4 (*Figure 7A*), similar to that seen in the wild-type. Accordingly, vernalization-triggered acceleration of flowering was comparable in the wild-type and *cbfs* (*Figure 7B-C*), indicating that *cbfs* show a normal vernalization response. It has recently been proposed that the strong induction of *COOLAIR* by the first seasonal frost is correlated with stronger *FLC* repression (*Zhao et al., 2021*). However, hyper-repression of *FLC* upon exposure to freezing temperature for 8 h after 20V (20V+8hF) was not observed under our growth conditions, in both the wild-type and *cbfs* (*Figure 7D*), although both genotypes showed stronger *COOLAIR* induction upon 8hF treatment (*Figure 4C*).

Since our results suggested that *COOLAIR* induction is not required for *FLC* silencing achieved by means of vernalization, we checked if the loss-of-function mutant, $FLC_{\Delta COOLAIR}$, displays any defect in the vernalization response. The $FLC_{\Delta COOLAIR}$ mutant produced virtually undetectable levels of total *COOLAIR* even after 20V (*Figure 5B*). Additionally, although the proximal *COOLAIR* variant was barely detected in $FLC_{\Delta COOLAIR}$ as previously reported (*Zhao et al., 2021*), the level of the proximal form did not increase by 20V (*Figure 5B*). Therefore, the results strongly suggested that $FLC_{\Delta COOLAIR}$ fails to show vernalization-induced *COOLAIR* expression. We then compared *FLC* levels between the wild-type and $FLC_{\Delta COOLAIR}$ after vernalization (*Figure 7E*). Similar to the wild-type, the *FLC* level gradually decreased and was silenced by long-term cold in $FLC_{\Delta COOLAIR}$. Consistently, the flowering time of $FLC_{\Delta COOLAIR}$ was normally accelerated by vernalization (*Figure 7F*). Taken together, it is likely that CBFs, upregulated by long-term cold, induce *COOLAIR* expression (*Figure 8*). However, such induced *COOLAIR* does not seem to be absolutely necessary for *FLC* silencing during vernalization.

Discussion

Plants recognize and remember a period of cold during the winter season to determine the proper timing of flowering. Several long-term cold-induced factors are known to facilitate such "memory of winter", which establishes flowering competence (*Michaels and Amasino, 2000; Sung and Amasino, 2004; Heo and Sung, 2011; Csorba et al., 2014; Kim and Sung, 2017b*). However, the mechanism by which long-term cold activates such regulators is not well understood. In the present study, we showed that CBF proteins act as transcriptional activators of *COOLAIR*, a long-term cold-induced lncRNA, during vernalization. CBF3 directly binds to the CRT/DRE elements located in the *COOLAIR* promoter region, which is evolutionarily conserved among *FLC* orthologs from Arabis family plants. CBFs are required for the full induction of *COOLAIR* during vernalization (*Figures 2C and 4A*), but their overexpression upregulates *COOLAIR* even at warm temperatures (*Figures 2A and 4B*). Consistently, our results show a gradual accumulation of CBFs during vernalization (*Figure 3*). Thus we propose that the increase in CBF levels induces *COOLAIR* expression during vernalization (*Figure 8*).

However, CBF-mediated *COOLAIR* induction during vernalization cannot be fully explained by increased CBF levels, as the *CBF3* overexpressor still shows *COOLAIR* induction by vernalization (*Figure 4B*). This suggests the involvement of additional factors that regulate CBF function. Previously, it has been reported that low temperatures cause functional activation of CBFs through degradation of HD2C and BTF3s, which prevent CBFs from activating downstream targets at warm temperatures (*Ding et al., 2018; Park et al., 2018*). Moreover, cold triggers the monomerization of CBF proteins, thereby activating their functions (*Lee et al., 2021*). Similarly, such an additional regulatory mechanism of CBFs, which fine-tunes vernalization-induced *COOLAIR* activation, may be enhanced by long-term winter cold. Additionally, *cbfs* mutant showed weak *COOLAIR* induction at 20V (*Figure 4A*). Thus, there are likely other thermosensors that facilitate *COOLAIR* induction by vernalization. Recently, it has been suggested that NTL8, an NAC domain-containing transcription factor, acts as an upstream regulator of *COOLAIR* (*Zhao et al., 2021*). NTL8 also binds to the *COOLAIR* promoter region, which is not far from the CBF-binding sites (*O'Malley et al., 2016; Zhao et al., 2021*). Furthermore, *COOLAIR* has been shown to be highly expressed in both dominant

330 mutant alleles, *ntl8-D*s, and *NTL8*-overexpressing transgenic plants at warm temperatures.
331 Thus, it has been proposed that slow accumulation of NTL8 protein, due to reduced dilution
332 resulting from slower growth at low temperatures, causes *COOLAIR* induction during
333 vernalization. It would be worthwhile to elucidate whether CBFs and NTL8 synergistically
334 activate *COOLAIR* transcription during vernalization. The reason as to why vernalization-
335 triggered *COOLAIR* induction requires more than one thermosensor is not apparent.
336 Presumably, multiple thermosensory modules ensure precise and robust *COOLAIR* expression
337 during the winter season when the temperature fluctuates.

338 The increasing trend of *COOLAIR* levels under long-term cold is not maintained across
339 the entire vernalization period (*Swiezewski et al., 2009; Csorba et al., 2014*). After reaching a
340 maximum at the early phase of vernalization, the *COOLAIR* level gradually reduced, although
341 the accumulation of CBFs continued as vernalization proceeded (*Figures 3 and 4A*). This is
342 likely due to the falling off of CBF proteins from the *COOLAIR* promoter during the late phase
343 of vernalization (*Figure 8*). The molecular mechanisms underlying this phenomenon are yet to
344 be explored. One possibility is that epigenetic silencing of *FLC*, which occurs after cold-
345 induced transcriptional silencing (*Antoniou-Kourounioti et al., 2018; Hepworth et al., 2018*),
346 suppresses both *COOLAIR* and *FLC*. A previous report has shown that there is a continuous
347 increase in the *COOLAIR* level throughout the vernalization period in the *vin3* mutant
348 (*Swiezewski et al., 2009*). Thus, VIN3-dependent polycomb silencing appears to be at least
349 partially involved in this mechanism.

350 Based on previous reports and the results shown here, CBFs are believed to facilitate both
351 sense and antisense transcription of *FLC,* depending on the duration of cold exposure (*Seo et*
352 *al., 2009*). Under intermittent cold, such as a brief cold treatment during daytime, CBFs activate
353 *FLC* expression, thus delaying floral transition (*Seo et al., 2009*). By contrast, under conditions
354 of long-term winter cold, CBFs favor *COOLAIR* activation over *FLC* transcription (*Figure 4*).
355 Considering that CBF3 protein is enriched at both the 5′- and 3′-ends of *FLC* under warm
356 conditions (*Figure 1C*), CBFs are likely to directly activate both sense and antisense
357 transcription of *FLC*. However, CBF3 enrichment at the 5′-end of *FLC* was quickly reduced to
358 the basal level by prolonged cold (*Figure 1C*), suggesting that CBF3 loses its control over *FLC*

359 transcription in the sense direction. By contrast, CBF3 protein binds to the *COOLAIR* promoter
360 during the early phase of vernalization, which leads to *COOLAIR* induction (*Figure 1C*). Thus,
361 we propose that different types of cold durations determine the direction of *FLC* transcription
362 by controlling the binding of CBF to the *FLC* locus. This may allow plants to flower in
363 favorable environments.

364 Extensive analyses of genes involved in AP have revealed how processing of proximal
365 *COOLAIR* is associated with switching *FLC* chromatin state inactive (*Whittaker and Dean,*
366 *2017; Wu et al., 2020*). Under warm temperatures, a group of AP proteins involved in RNA 3′-
367 end processing, such as FCA, FY, FPA, CLEAVAGE STIMULATION FACTOR 64 (CstF64),
368 and CstF77, promote proximal polyadenylation of *COOLAIR* (*Hornyik et al., 2010; Liu et al.,*
369 *2010*). This process is linked to H3K4 demethylation at the *FLC* locus through the interaction
370 of FCA and FLOWERING LOCUS D (FLD), an AP protein that acts as an H3K4 demethylase,
371 thus suppressing *FLC* (*Liu et al., 2010*). In contrast with such a role of *COOLAIR* for *FLC*
372 repression at warm temperatures, there is some controversy regarding the function of
373 *COOLAIR* in vernalization-induced epigenetic silencing of *FLC* (*Swiezewski et al., 2009;*
374 *Helliwell et al., 2011; Li et al., 2018; Luo et al., 2019; Luo and He, 2020; Zhao et al., 2021*).
375 The results shown here favor the proposal that *COOLAIR* expression is not required for
376 vernalization response. The *cbfs* mutant, which exhibited severely reduced *COOLAIR*
377 induction, showed almost normal vernalization responses such that flowering time is fairly well
378 accelerated and active histone marks, H3K36me3 and H3K4me3, are reduced, but inactive
379 histone mark, H3K27me3, is increased on the *FLC* chromatin by vernalization as seen in the
380 wild-type (*Figures 6 and 7*). Consistently, the $FLC_{\Delta COOLAIR}$ mutant, which had almost
381 undetectable levels of total *COOLAIR* and failed to induce proximal *COOLAIR* by
382 vernalization, showed both *FLC* suppression and acceleration of flowering by vernalization
383 similar to that seen in the wild-type (*Figure 7*). Moreover, the freezing temperature treatment
384 mimicking the first frost did not affect *FLC* suppression, although it caused CBF-mediated
385 *COOLAIR* induction, as reported previously (*Figures 4C and 7D; Zhao et al., 2021*). It is
386 noteworthy that our hypothesis, favoring against *FLC* suppression mediated by vernalization-
387 induced *COOLAIR,* has been formulated using mutant lines, *cbfs* and $FLC_{\Delta COOLAIR}$, instead of
388 transgenic lines. Thus, we could exclude the possibility that transgenes somehow affect the

389 vernalization response.

390 This discrepancy can be explained in several ways. First, different experimental schemes
391 may affect the vernalization response differently. The *bona fide* evidence favoring the
392 hypothesis that vernalization-induced *COOLAIR* acts on *FLC* suppression has been obtained
393 in natural environments with fluctuating temperatures (*Zhao et al., 2021*). However, most of
394 the experiments in previous studies were performed in constant environments. Thus, it is
395 possible that fluctuating temperatures have different effects on the vernalization response.
396 Consistent with such idea, in our experiment using the first frost-mimicking cold treatment,
397 *FLC* suppression was not observed, although *COOLAIR* was strongly activated, as reported
398 (*Zhao et al., 2021*). The difference between the two experimental schemes is fluctuating versus
399 constant cold conditions. The other reason may be due to the small level of CAS (convergent
400 antisense transcript of *COOLAIR*) produced at the 5′-end of *FLC* in transgenic lines defective
401 of *COOLAIR* promoter or even in the $FLC_{\Delta COOLAIR}$ mutant (*Zhao et al., 2021*), which may
402 somehow affect the epigenetic silencing of *FLC*. Otherwise, the effect of *COOLAIR* on *FLC*
403 silencing may be obscured due to the functional redundancy between *COOLAIR* and other
404 lncRNA, such as *COLDAIR* in Arabidopsis, as suggested previously (*Castaings et al., 2014*).

405 Although cold stress and vernalization elicit different developmental responses, both are
406 triggered by the same physical environment. Therefore, it is logical that a common signaling
407 network governs both the processes. *CBF* genes have been highlighted for their role in cold
408 stress responses (*Gilmour et al., 1998; Liu et al., 1998; Jia et al., 2016; Zhao et al., 2016*).
409 CBFs rapidly accumulate upon short-term cold exposure, thereby activating the transcription
410 of cold-responsive genes, such as *COR15A* and *RD29A* (*Stockinger et al., 1997; Liu et al.,*
411 *1998*). Interestingly, CBFs are also highly accumulated during the vernalization process and
412 mediate long-term cold-induced *COOLAIR* expression. Hence, our results support that cold
413 signaling and vernalization pathways are not sharply distinguishable, as suggested previously
414 (*Seo et al., 2009*).

415 **Materials and Methods**

416 **Plant materials and treatments**

417 *Arabidopsis thaliana* Columbia-0 (Col-0), Wassilewskija-2 (Ws-2), and Col:*FRI*^{SF2} (*FRI* Col)
418 were used as wild types in this study. "Wild type" in this paper mainly refers to *FRI* Col unless
419 otherwise specified. *FRI* Col (*Lee et al., 1994*), *cbfs-1*, *pCBF3::CBF3-myc* (*Jia et al., 2016*),
420 *pSuper::CBF3-myc* (*Liu et al., 2017*), *35S::CBF1*, *35S::CBF2*, and *35S::CBF3* (*Gilmour et al.,*
421 *2004*) have previously been described. *FRI cbfs-1* was generated by crossing *FRI* Col with
422 *cbfs-1* stated above. $FLC_{\Delta COOLAIR}$ was generated by crossing *FRI* Col with $FLC_{\Delta COOLAIR}$ in Col-
423 0 background described previously (*Luo et al., 2019*). For all experiments using plant materials,
424 seeds were sown on half-strength Murashige & Skoog (MS) media (Duchefa) containing 1%
425 sucrose and 1% plant agar (Duchefa) and stratified at 4°C for 3 days. Plants were germinated
426 and grown at 22ºC under a short day (SD) cycle (8 h light/16 h dark) with cool white fluorescent
427 lights (100 μmol m^{-2} s^{-1}). For the vernalization treatment, plants were grown at 22ºC for the
428 prescribed period and then transferred to a 4ºC growth chamber under an SD cycle. To adjust
429 the developmental stage, the plants to be vernalized for 40 days (40V), 30 days (30V), 20 days
430 (20V), 10 days (10V), and 1 day (1V) were transferred to 4ºC after being grown at 22ºC for 10
431 days, 12 days, 14 days, 15 days, and 16 days respectively. Non-vernalized (NV) plants were
432 grown at 22ºC for 16 days. For 0. 0.5, 1, 1.5, 2, 3, 6, and 24 hours of cold treatment, plants
433 were grown at 22ºC for 16 days before the 4ºC treatment. For the freezing treatment, 20V plants
434 were transferred to –1ºC, dark condition for 8 hours (8hF). To measure flowering time of
435 vernalized plants, plants were transferred to 22ºC under a long day (LD) cycle (16 h light/8 h
436 dark) directly after the vernalization treatment.

437

438 **Plasmid construction**

439 To generate the *35S::CBF3-HA* construct, the entire coding sequence of *CBF3* was amplified
440 by PCR and was cloned into the *HBT-HA-NOS* plasmid (*Yoo et al., 2007*). For
441 $pCOOLAIR_{DRE}$*::LUC* and $pCOOLAIR_{DRE}{}^{m}$*::LUC* construction, the 1 kb sequence containing
442 the *COOLAIR* promoter, the 3' UTR and last exon of *FLC* was amplified by PCR and was

443 cloned into *LUC-NOS* plasmid (*Hwang and Sheen, 2001*). To generate *pCOOLAIR*$_{DRE}^{m}$*::LUC,*
444 two CRT/DREs in the *COOLAIR* promoter, 5'-AGGTCGGT-3' and 5'-ACCGACAT-3', were
445 replaced with 5'-CGAGGTGT-3' and 5'-TGAACCCA-3', respectively. For *pFLC::LUC*
446 construction, the 1 kb sequence containing the promoter, 5' UTR, and first exon of *FLC* was
447 amplified by PCR and was cloned into the *LUC-NOS* plasmid.

448

449 **Electrophoretic mobility shift assay (EMSA)**

450 Maltose binding protein (MBP) and MBP-CBF3 recombinant fusion protein were induced by
451 500 μM of isopropyl β-D-thiogalactoside (IPTG) in *E. coli* BL21 (DE3) strain. Cell extracts
452 were isolated with buffer containing 20 mM Tris-HCl (pH 7.4), 1 mM EDTA, 200 mM NaCl,
453 10% Glycerol, 1 mM DTT, and 1 mM PMSF. Proteins were purified from cell extracts using
454 MBPTrap™ HP column (GE Healthcare) with ÄKTA FPLC system (Amersham Biosciences).
455 The Cy5-labelled probes and unlabelled competitors were generated by annealing 25 bp-length
456 oligonucleotides. EMSA was performed as previously described with few modifications (*Seo*
457 *et al., 2012*). 5 μM of proteins and 100 nM of Cy5-labelled probe were incubated together at
458 room temperature in a binding buffer containing 10 mM Tris-HCl (pH 7.5), 1 mM EDTA, 50
459 mM NaCl, 5% glycerol, and 5 mM DTT for each EMSA reaction. For the competition assay,
460 the reaction mixtures were incubated in the presence of 100-fold molar excess of each
461 competitor. The reaction mixtures were electrophoresed at 100 V after incubation. The Cy5
462 signals were detected using WSE-6200H LuminoGraph II (ATTO).

463

464 **Chromatin immunoprecipitation (ChIP) assay**

465 Approximately 4 g of seedlings grown on MS plate were collected and cross-linked using 1%
466 (v/v) formaldehyde. Nuclei were isolated from seedlings using buffer containing 20 mM
467 PIPES-KOH pH 7.6, 1 M hexylene glycol, 10 mM MgCl2, 0.1 mM EGTA, 15 mM NaCl, 60
468 mM KCl, 0.5% Triton-X, 5 mM β-mercaptoethanol, and 1X cOmplete™ EDTA-free Protease
469 Inhibitor Cocktail (Roche) as described previously with few modifications (*Shu et al., 2014*).
470 Isolated nuclei were lysed with buffer containing 50 mM Tris-HCl (pH 7.4), 150 mM NaCl, 1%

471 (v/v) Triton X-100, and 1% SDS (w/v), and were subsequently sonicated using Digital
472 Sonifier® (Branson). Sheared chromatin was diluted with buffer containing 50 mM Tris-HCl
473 (pH 7.4), 150 mM NaCl, 1% (v/v) Triton X-100, and 1 mM EDTA. Immunoprecipitation was
474 undertaken by incubating sheared chromatin together with Protein G Sepharose™ 4 Fast Flow
475 beads (GE Healthcare) and antibodies. Anti-myc (MBL, #M192-3) and normal mouse IgG_1
476 (Santa Cruz, #sc-3877) were used to detect CBF3 protein enrichment on *FLC* locus, and anti-
477 H3K36me3 (Abcam, #Ab9050), H3K4me3 (Millipore, #07-473), and anti-H3K27me3
478 (Millipore, #07-449) were used to detect histone modifications deposited on *FLC* chromatin.
479 DNA was extracted with phenol:chloroform:isoamyl alcohol (25:24:1, v/v) or with Chelex®
480 100 Resin according to the manufacturer's instruction.

481

482 **Gene expression analysis**

483 Total RNA was isolated from ~100 mg of seedlings grown on MS agar plate using TRI
484 Reagent® (Sigma-Aldrich) or TS™ Plant Mini Kit (Taeshin Bio Science, Gyeonggi-do,
485 Republic of Korea). cDNA was generated using 4 μg of total RNA, 5 units of Recombinant
486 DNase I (TaKaRa), 200 units of RevertAid™ Reverse Transcriptase (Thermo Scientific), and
487 buffer containing 0.25 mM dNTP and 0.1 μg oligo$(dT)_{18}$. Quantitative PCR analysis was
488 performed using iQ™ SYBR® Green Supermix (Bio-Rad) and CFX96 Real-Time PCR system
489 (Bio-Rad).

490

491 **Immunoblotting**

492 Total protein was isolated from ~100 mg of seedlings using buffer containing 50 mM Tris-HCl
493 (pH 7.5), 100 mM NaCl, 10 mM $MgCl_2$, 1 mM EDTA, 10% glycerol, 1 mM PMSF, 1 mM DTT
494 and the 1X cOmplete™ EDTA-free Protease Inhibitor Cocktail (Roche). 50 μg of total protein
495 was loaded onto SDS-PAGE gels and separated by electrophoresis. The proteins were
496 transferred to PVDF membranes (Amersham Biosciences) and probed with anti-myc (MBL,
497 #M192-3; 1:10000 dilution) antibody overnight at 4°C. Then, the samples were probed with
498 horseradish peroxidase (HRP)-conjugated anti-mouse IgG (Cell Signaling, #7076; 1:10000

499 dilution) antibody at room temperature. The signals were detected by ImageQuant™ LAS 4000
500 (GE Healthcare) using WesternBright™ Sirius ECL solution (Advansta).

501

502 **Luciferase assay using Arabidopsis protoplast**

503 Protoplast isolation and transfection were undertaken as previously described with few
504 modifications (*Yoo et al., 2007*). Protoplast was isolated from leaves of SD-grown wild-type
505 plant (Col-0) using a buffer containing 150 mg Cellulase Onozuka™ R-10 (Yakult), 50 mg
506 Maceroenzyme™ R-10 (Yakult), 20 mM KCl, 20 mM MES-KOH (pH 5.6), 0.4 M D-mannitol,
507 10 mM $CaCl_2$, 5 mM β-mercaptoethanol, 0.1 g bovine serum albumin. For protoplast
508 transfection, 200 μg of plasmid DNA and isolated protoplast were incubated together in buffer
509 containing 0.1 M D-mannitol, 50 mM $CaCl_2$, and 20% (w/v) PEG. Luciferase activity in
510 protoplast was measured using Luciferase Assay System (Promega) and MicroLumat Plus
511 LB96V microplate luminometer (Berthold Technologies).

512

513

514 **Acknowledgements**

515 We would like to thank Dr. Shuhua Yang (China Agricultural University, China) for providing
516 *cbfs-1*, *pSuper::CBF3-myc* and *pCBF3::CBF3-myc* seeds, and Dr. Yuehui He (Peking
517 University, China) for providing $FLC_{\Delta COOLAIR}$ seeds. This work was carried out with the support
518 of Cooperative Research Program for Agriculture Science and Technology Development (No.
519 PJ01315201 and PJ01315401), Rural Development Administration, Republic of Korea, and of
520 the National Research Foundation of Korea (NRF) grant funded by the Korea government
521 (MSIT) (No. 2019R1A2C2004313). This work was also supported by NRF grant funded by
522 the Ministry of Science, Republic of Korea (NRF-2021R1A5A1032428). M. Jeon was
523 supported by Brain Korea 21 Plus Project of the NRF grant.

524

525

Competing interests

The authors declare that no competing interests exist.

Supplementary Files

Supplementary File 1. Oligonucleotide sequences used in this study.

References

Angel, A, Song, J, Dean, C, Howard, M. 2011. A Polycomb-based switch underlying quantitative epigenetic memory. *Nature* **476:** 105-108. DOI: https://doi.org/10.1038/nature10241

Antoniou-Kourounioti, RL, Hepworth, J, Heckmann, A, Duncan, S, Questa, J, Rosa, S, Sall, T, Holm, S, Dean, C, Howard, M. 2018. Temperature Sensing Is Distributed throughout the Regulatory Network that Controls FLC Epigenetic Silencing in Vernalization. *Cell Syst* **7:** 643-655 e649. DOI: https://doi.org/10.1016/j.cels.2018.10.011

Baker, SS, Wilhelm, KS, Thomashow, MF. 1994. The 5'-region of Arabidopsis thaliana cor15a has cis-acting elements that confer cold-, drought- and ABA-regulated gene expression. *Plant Mol Biol* **24:** 701-713. DOI: https://doi.org/10.1007/BF00029852

Bastow, R, Mylne, JS, Lister, C, Lippman, Z, Martienssen, RA, Dean, C. 2004. Vernalization requires epigenetic silencing of FLC by histone methylation. *Nature* **427:** 164-167. DOI: https://doi.org/10.1038/nature02269

Berry, S, Dean, C. 2015. Environmental perception and epigenetic memory: mechanistic insight through FLC. *Plant J* **83:** 133-148. DOI: https://doi.org/10.1111/tpj.12869

Castaings, L, Bergonzi, S, Albani, MC, Kemi, U, Savolainen, O, Coupland, G. 2014. Evolutionary conservation of cold-induced antisense RNAs of FLOWERING LOCUS C in Arabidopsis thaliana perennial relatives. *Nat Commun* **5:** 4457. DOI: https://doi.org/10.1038/ncomms5457

Choi, K, Kim, J, Hwang, HJ, Kim, S, Park, C, Kim, SY, Lee, I. 2011. The FRIGIDA complex activates transcription of FLC, a strong flowering repressor in Arabidopsis, by recruiting chromatin modification factors. *Plant Cell* **23:** 289-303. DOI: https://doi.org/10.1105/tpc.110.075911

Chouard, P. 1960. Vernalization and Its Relations to Dormancy. *Annual Review of Plant Physiology and Plant Molecular Biology* **11:** 191-238. DOI: https://doi.org/DOI 10.1146/annurev.pp.11.060160.001203

Clarke, JH, Dean, C. 1994. Mapping FRI, a locus controlling flowering time and vernalization response in Arabidopsis thaliana. *Mol Gen Genet* **242:** 81-89. DOI: https://doi.org/10.1007/BF00277351

Csorba, T, Questa, JI, Sun, Q, Dean, C. 2014. Antisense COOLAIR mediates the coordinated switching of chromatin states at FLC during vernalization. *Proc Natl Acad Sci U S A* **111:** 16160-16165. DOI: https://doi.org/10.1073/pnas.1419030111

De Lucia, F, Crevillen, P, Jones, AM, Greb, T, Dean, C. 2008. A PHD-polycomb repressive complex 2 triggers the epigenetic silencing of FLC during vernalization. *Proc Natl Acad Sci U S A* **105:** 16831-16836. DOI: https://doi.org/10.1073/pnas.0808687105

Ding, Y, Jia, Y, Shi, Y, Zhang, X, Song, C, Gong, Z, Yang, S. 2018. OST1-mediated BTF3L

570 phosphorylation positively regulates CBFs during plant cold responses. *EMBO J* **37**.
571 DOI: https://doi.org/10.15252/embj.201798228
572 **Dong, MA, Farre, EM, Thomashow, MF.** 2011. Circadian clock-associated 1 and late
573 elongated hypocotyl regulate expression of the C-repeat binding factor (CBF) pathway
574 in Arabidopsis. *Proc Natl Acad Sci U S A* **108:** 7241-7246. DOI:
575 https://doi.org/10.1073/pnas.1103741108
576 **Fowler, S, Thomashow, MF.** 2002. Arabidopsis transcriptome profiling indicates that multiple
577 regulatory pathways are activated during cold acclimation in addition to the CBF cold
578 response pathway. *Plant Cell* **14:** 1675-1690. DOI:
579 https://doi.org/10.1105/tpc.003483
580 **Gazzani, S, Gendall, AR, Lister, C, Dean, C.** 2003. Analysis of the molecular basis of
581 flowering time variation in Arabidopsis accessions. *Plant Physiol* **132:** 1107-1114.
582 DOI: https://doi.org/10.1104/pp.103.021212
583 **Gilmour, SJ, Fowler, SG, Thomashow, MF.** 2004. Arabidopsis transcriptional activators
584 CBF1, CBF2, and CBF3 have matching functional activities. *Plant Mol Biol* **54:**
585 767-781. DOI: https://doi.org/10.1023/B:PLAN.0000040902.06881.d4
586 **Gilmour, SJ, Zarka, DG, Stockinger, EJ, Salazar, MP, Houghton, JM, Thomashow, MF.**
587 1998. Low temperature regulation of the Arabidopsis CBF family of AP2
588 transcriptional activators as an early step in cold-induced COR gene expression. *Plant*
589 *J* **16:** 433-442. DOI: https://doi.org/10.1046/j.1365-313x.1998.00310.x
590 **Helliwell, CA, Robertson, M, Finnegan, EJ, Buzas, DM, Dennis, ES.** 2011. Vernalization-
591 repression of Arabidopsis FLC requires promoter sequences but not antisense
592 transcripts. *PLoS One* **6:** e21513. DOI:
593 https://doi.org/10.1371/journal.pone.0021513
594 **Helliwell, CA, Wood, CC, Robertson, M, James Peacock, W, Dennis, ES.** 2006. The
595 Arabidopsis FLC protein interacts directly in vivo with SOC1 and FT chromatin and is
596 part of a high-molecular-weight protein complex. *Plant J* **46:** 183-192. DOI:
597 https://doi.org/10.1111/j.1365-313X.2006.02686.x
598 **Heo, JB, Sung, S.** 2011. Vernalization-mediated epigenetic silencing by a long intronic
599 noncoding RNA. *Science* **331:** 76-79. DOI:
600 https://doi.org/10.1126/science.1197349
601 **Hepworth, J, Antoniou-Kourounioti, RL, Bloomer, RH, Selga, C, Berggren, K, Cox, D,**
602 **Collier Harris, BR, Irwin, JA, Holm, S, Sall, T, Howard, M, Dean, C.** 2018. Absence
603 of warmth permits epigenetic memory of winter in Arabidopsis. *Nat Commun* **9:**
604 639. DOI: https://doi.org/10.1038/s41467-018-03065-7
605 **Hornyik, C, Duc, C, Rataj, K, Terzi, LC, Simpson, GG.** 2010. Alternative polyadenylation
606 of antisense RNAs and flowering time control. *Biochem Soc Trans* **38:** 1077-1081.
607 DOI: https://doi.org/10.1042/BST0381077
608 **Hwang, I, Sheen, J.** 2001. Two-component circuitry in Arabidopsis cytokinin signal

609 transduction. *Nature* **413:** 383-389. DOI: https://doi.org/10.1038/35096500
610 **Jia, Y, Ding, Y, Shi, Y, Zhang, X, Gong, Z, Yang, S.** 2016. The cbfs triple mutants reveal the
611 essential functions of CBFs in cold acclimation and allow the definition of CBF
612 regulons in Arabidopsis. *New Phytol* **212:** 345-353. DOI:
613 https://doi.org/10.1111/nph.14088
614 **Johanson, U, West, J, Lister, C, Michaels, S, Amasino, R, Dean, C.** 2000. Molecular analysis
615 of FRIGIDA, a major determinant of natural variation in Arabidopsis flowering time.
616 *Science* **290:** 344-347. DOI: https://doi.org/10.1126/science.290.5490.344
617 **Kim, DH, Sung, S.** 2013. Coordination of the vernalization response through a VIN3 and FLC
618 gene family regulatory network in Arabidopsis. *Plant Cell* **25:** 454-469. DOI:
619 https://doi.org/10.1105/tpc.112.104760
620 **Kim, DH, Sung, S.** 2017a. The Binding Specificity of the PHD-Finger Domain of VIN3
621 Moderates Vernalization Response. *Plant Physiol* **173:** 1258-1268. DOI:
622 https://doi.org/10.1104/pp.16.01320
623 **Kim, DH, Sung, S.** 2017b. Vernalization-Triggered Intragenic Chromatin Loop Formation by
624 Long Noncoding RNAs. *Dev Cell* **40:** 302-312 e304. DOI:
625 https://doi.org/10.1016/j.devcel.2016.12.021
626 **Koornneef, M, Alonso-Blanco, C, Blankestijn-de Vries, H, Hanhart, CJ, Peeters, AJ.** 1998.
627 Genetic interactions among late-flowering mutants of Arabidopsis. *Genetics* **148:**
628 885-892.
629 **Koornneef, M, Blankestijndevries, H, Hanhart, C, Soppe, W, Peeters, T.** 1994. The
630 Phenotype of Some Late-Flowering Mutants Is Enhanced by a Locus on Chromosome-
631 5 That Is Not Effective in the Landsberg Erecta Wild-Type. *Plant Journal* **6:** 911-
632 919. DOI: https://doi.org/DOI 10.1046/j.1365-313X.1994.6060911.x
633 **Lee, ES, Park, JH, Wi, SD, Kang, CH, Chi, YH, Chae, HB, Paeng, SK, Ji, MG, Kim, WY,**
634 **Kim, MG, Yun, DJ, Stacey, G, Lee, SY.** 2021. Redox-dependent structural switch and
635 CBF activation confer freezing tolerance in plants. *Nat Plants* **7:** 914-922. DOI:
636 https://doi.org/10.1038/s41477-021-00944-8
637 **Lee, H, Suh, SS, Park, E, Cho, E, Ahn, JH, Kim, SG, Lee, JS, Kwon, YM, Lee, I.** 2000.
638 The AGAMOUS-LIKE 20 MADS domain protein integrates floral inductive pathways
639 in Arabidopsis. *Genes Dev* **14:** 2366-2376. DOI:
640 https://doi.org/10.1101/gad.813600
641 **Lee, I, Bleecker, A, Amasino, R.** 1993. Analysis of naturally occurring late flowering in
642 Arabidopsis thaliana. *Mol Gen Genet* **237:** 171-176. DOI:
643 https://doi.org/10.1007/BF00282798
644 **Lee, I, Michaels, SD, Masshardt, AS, Amasino, RM.** 1994. The Late-Flowering Phenotype
645 of Frigida and Mutations in Luminidependens Is Suppressed in the Landsberg Erecta
646 Strain of Arabidopsis. *Plant Journal* **6:** 903-909. DOI: https://doi.org/DOI
647 10.1046/j.1365-313X.1994.6060903.x

Li, Z, Jiang, D, He, Y. 2018. FRIGIDA establishes a local chromosomal environment for FLOWERING LOCUS C mRNA production. *Nat Plants* **4:** 836-846. DOI: https://doi.org/10.1038/s41477-018-0250-6

Liu, F, Marquardt, S, Lister, C, Swiezewski, S, Dean, C. 2010. Targeted 3' processing of antisense transcripts triggers Arabidopsis FLC chromatin silencing. *Science* **327:** 94-97. DOI: https://doi.org/10.1126/science.1180278

Liu, Q, Kasuga, M, Sakuma, Y, Abe, H, Miura, S, Yamaguchi-Shinozaki, K, Shinozaki, K. 1998. Two transcription factors, DREB1 and DREB2, with an EREBP/AP2 DNA binding domain separate two cellular signal transduction pathways in drought- and low-temperature-responsive gene expression, respectively, in Arabidopsis. *Plant Cell* **10:** 1391-1406. DOI: https://doi.org/10.1105/tpc.10.8.1391

Liu, Z, Jia, Y, Ding, Y, Shi, Y, Li, Z, Guo, Y, Gong, Z, Yang, S. 2017. Plasma Membrane CRPK1-Mediated Phosphorylation of 14-3-3 Proteins Induces Their Nuclear Import to Fine-Tune CBF Signaling during Cold Response. *Mol Cell* **66:** 117-128 e115. DOI: https://doi.org/10.1016/j.molcel.2017.02.016

Luo, X, Chen, T, Zeng, X, He, D, He, Y. 2019. Feedback Regulation of FLC by FLOWERING LOCUS T (FT) and FD through a 5' FLC Promoter Region in Arabidopsis. *Mol Plant* **12:** 285-288. DOI: https://doi.org/10.1016/j.molp.2019.01.013

Luo, X, He, Y. 2020. Experiencing winter for spring flowering: A molecular epigenetic perspective on vernalization. *J Integr Plant Biol* **62:** 104-117. DOI: https://doi.org/10.1111/jipb.12896

Marquardt, S, Raitskin, O, Wu, Z, Liu, F, Sun, Q, Dean, C. 2014. Functional consequences of splicing of the antisense transcript COOLAIR on FLC transcription. *Mol Cell* **54:** 156-165. DOI: https://doi.org/10.1016/j.molcel.2014.03.026

Maruyama, K, Sakuma, Y, Kasuga, M, Ito, Y, Seki, M, Goda, H, Shimada, Y, Yoshida, S, Shinozaki, K, Yamaguchi-Shinozaki, K. 2004. Identification of cold-inducible downstream genes of the Arabidopsis DREB1A/CBF3 transcriptional factor using two microarray systems. *Plant J* **38:** 982-993. DOI: https://doi.org/10.1111/j.1365-313X.2004.02100.x

McKhann, HI, Gery, C, Berard, A, Leveque, S, Zuther, E, Hincha, DK, De Mita, S, Brunel, D, Teoule, E. 2008. Natural variation in CBF gene sequence, gene expression and freezing tolerance in the Versailles core collection of Arabidopsis thaliana. *BMC Plant Biol* **8:** 105. DOI: https://doi.org/10.1186/1471-2229-8-105

Medina, J, Bargues, M, Terol, J, Perez-Alonso, M, Salinas, J. 1999. The Arabidopsis CBF gene family is composed of three genes encoding AP2 domain-containing proteins whose expression Is regulated by low temperature but not by abscisic acid or dehydration. *Plant Physiol* **119:** 463-470. DOI: https://doi.org/10.1104/pp.119.2.463

Michaels, SD, Amasino, RM. 1999. FLOWERING LOCUS C encodes a novel MADS

687 domain protein that acts as a repressor of flowering. *Plant Cell* **11:** 949-956. DOI:
688 https://doi.org/10.1105/tpc.11.5.949
689 **Michaels, SD, Amasino, RM.** 2000. Memories of winter: vernalization and the competence to
690 flower. *Plant Cell and Environment* **23:** 1145-1153. DOI: https://doi.org/DOI
691 10.1046/j.1365-3040.2000.00643.x
692 **Michaels, SD, Amasino, RM.** 2001. Loss of FLOWERING LOCUS C activity eliminates the
693 late-flowering phenotype of FRIGIDA and autonomous pathway mutations but not
694 responsiveness to vernalization. *Plant Cell* **13:** 935-941. DOI:
695 https://doi.org/10.1105/tpc.13.4.935
696 **Michaels, SD, He, Y, Scortecci, KC, Amasino, RM.** 2003. Attenuation of FLOWERING
697 LOCUS C activity as a mechanism for the evolution of summer-annual flowering
698 behavior in Arabidopsis. *Proc Natl Acad Sci U S A* **100:** 10102-10107. DOI:
699 https://doi.org/10.1073/pnas.1531467100
700 **Michaels, SD, Himelblau, E, Kim, SY, Schomburg, FM, Amasino, RM.** 2005. Integration
701 of flowering signals in winter-annual Arabidopsis. *Plant Physiol* **137:** 149-156.
702 DOI: https://doi.org/10.1104/pp.104.052811
703 **Mylne, JS, Barrett, L, Tessadori, F, Mesnage, S, Johnson, L, Bernatavichute, YV,**
704 **Jacobsen, SE, Fransz, P, Dean, C.** 2006. LHP1, the Arabidopsis homologue of
705 HETEROCHROMATIN PROTEIN1, is required for epigenetic silencing of FLC. *Proc*
706 *Natl Acad Sci U S A* **103:** 5012-5017. DOI:
707 https://doi.org/10.1073/pnas.0507427103
708 **Napp-Zinn, K.** 1955. Genetische Grundlagen des Kältebedürfnisses beiArabidopsis thaliana
709 (L.) HEYNH. *Die Naturwissenschaften* **42:** 650. DOI:
710 https://doi.org/10.1007/BF00622395
711 **Novillo, F, Medina, J, Salinas, J.** 2007. Arabidopsis CBF1 and CBF3 have a different function
712 than CBF2 in cold acclimation and define different gene classes in the CBF regulon.
713 *Proc Natl Acad Sci U S A* **104:** 21002-21007. DOI:
714 https://doi.org/10.1073/pnas.0705639105
715 **O'Malley, RC, Huang, SC, Song, L, Lewsey, MG, Bartlett, A, Nery, JR, Galli, M,**
716 **Gallavotti, A, Ecker, JR.** 2016. Cistrome and Epicistrome Features Shape the
717 Regulatory DNA Landscape. *Cell* **166:** 1598. DOI:
718 https://doi.org/10.1016/j.cell.2016.08.063
719 **Park, J, Lim, CJ, Shen, M, Park, HJ, Cha, JY, Iniesto, E, Rubio, V, Mengiste, T, Zhu, JK,**
720 **Bressan, RA, Lee, SY, Lee, BH, Jin, JB, Pardo, JM, Kim, WY, Yun, DJ.** 2018.
721 Epigenetic switch from repressive to permissive chromatin in response to cold stress.
722 *Proc Natl Acad Sci U S A* **115:** E5400-E5409. DOI:
723 https://doi.org/10.1073/pnas.1721241115
724 **Park, S, Lee, CM, Doherty, CJ, Gilmour, SJ, Kim, Y, Thomashow, MF.** 2015. Regulation
725 of the Arabidopsis CBF regulon by a complex low-temperature regulatory network.

Plant J **82:** 193-207. DOI: https://doi.org/10.1111/tpj.12796

Seo, E, Lee, H, Jeon, J, Park, H, Kim, J, Noh, YS, Lee, I. 2009. Crosstalk between cold response and flowering in Arabidopsis is mediated through the flowering-time gene SOC1 and its upstream negative regulator FLC. *Plant Cell* **21:** 3185-3197. DOI: https://doi.org/10.1105/tpc.108.063883

Seo, PJ, Park, MJ, Lim, MH, Kim, SG, Lee, M, Baldwin, IT, Park, CM. 2012. A self-regulatory circuit of CIRCADIAN CLOCK-ASSOCIATED1 underlies the circadian clock regulation of temperature responses in Arabidopsis. *Plant Cell* **24:** 2427-2442. DOI: https://doi.org/10.1105/tpc.112.098723

Sheldon, CC, Burn, JE, Perez, PP, Metzger, J, Edwards, JA, Peacock, WJ, Dennis, ES. 1999. The FLF MADS box gene: a repressor of flowering in Arabidopsis regulated by vernalization and methylation. *Plant Cell* **11:** 445-458. DOI: https://doi.org/10.1105/tpc.11.3.445

Sheldon, CC, Rouse, DT, Finnegan, EJ, Peacock, WJ, Dennis, ES. 2000. The molecular basis of vernalization: the central role of FLOWERING LOCUS C (FLC). *Proc Natl Acad Sci U S A* **97:** 3753-3758. DOI: https://doi.org/10.1073/pnas.060023597

Shu, H, Nakamura, M, Siretskiy, A, Borghi, L, Moraes, I, Wildhaber, T, Gruissem, W, Hennig, L. 2014. Arabidopsis replacement histone variant H3.3 occupies promoters of regulated genes. *Genome Biol* **15:** R62. DOI: https://doi.org/10.1186/gb-2014-15-4-r62

Stockinger, EJ, Gilmour, SJ, Thomashow, MF. 1997. Arabidopsis thaliana CBF1 encodes an AP2 domain-containing transcriptional activator that binds to the C-repeat/DRE, a cis-acting DNA regulatory element that stimulates transcription in response to low temperature and water deficit. *Proc Natl Acad Sci U S A* **94:** 1035-1040. DOI: https://doi.org/10.1073/pnas.94.3.1035

Sung, S, Amasino, RM. 2004. Vernalization in Arabidopsis thaliana is mediated by the PHD finger protein VIN3. *Nature* **427:** 159-164. DOI: https://doi.org/10.1038/nature02195

Swiezewski, S, Liu, F, Magusin, A, Dean, C. 2009. Cold-induced silencing by long antisense transcripts of an Arabidopsis Polycomb target. *Nature* **462:** 799-802. DOI: https://doi.org/10.1038/nature08618

Tian, Y, Zheng, H, Zhang, F, Wang, S, Ji, X, Xu, C, He, Y, Ding, Y. 2019. PRC2 recruitment and H3K27me3 deposition at FLC require FCA binding of COOLAIR. *Sci Adv* **5:** eaau7246. DOI: https://doi.org/10.1126/sciadv.aau7246

Whittaker, C, Dean, C. 2017. The FLC Locus: A Platform for Discoveries in Epigenetics and Adaptation. *Annu Rev Cell Dev Biol* **33:** 555-575. DOI: https://doi.org/10.1146/annurev-cellbio-100616-060546

Wood, CC, Robertson, M, Tanner, G, Peacock, WJ, Dennis, ES, Helliwell, CA. 2006. The Arabidopsis thaliana vernalization response requires a polycomb-like protein complex

765 that also includes VERNALIZATION INSENSITIVE 3. *Proc Natl Acad Sci U S A*
766 **103:** 14631-14636. DOI: https://doi.org/10.1073/pnas.0606385103
767 **Wu, Z, Fang, X, Zhu, D, Dean, C.** 2020. Autonomous Pathway: FLOWERING LOCUS C
768 Repression through an Antisense-Mediated Chromatin-Silencing Mechanism. *Plant*
769 *Physiol* **182:** 27-37. DOI: https://doi.org/10.1104/pp.19.01009
770 **Yang, H, Berry, S, Olsson, TSG, Hartley, M, Howard, M, Dean, C.** 2017. Distinct phases
771 of Polycomb silencing to hold epigenetic memory of cold in Arabidopsis. *Science* **357:**
772 1142-1145. DOI: https://doi.org/10.1126/science.aan1121
773 **Yang, H, Howard, M, Dean, C.** 2014. Antagonistic roles for H3K36me3 and H3K27me3 in
774 the cold-induced epigenetic switch at Arabidopsis FLC. *Curr Biol* **24:** 1793-1797.
775 DOI: https://doi.org/10.1016/j.cub.2014.06.047
776 **Yoo, SD, Cho, YH, Sheen, J.** 2007. Arabidopsis mesophyll protoplasts: a versatile cell system
777 for transient gene expression analysis. *Nat Protoc* **2:** 1565-1572. DOI:
778 https://doi.org/10.1038/nprot.2007.199
779 **Zhao, C, Zhang, Z, Xie, S, Si, T, Li, Y, Zhu, JK.** 2016. Mutational Evidence for the Critical
780 Role of CBF Transcription Factors in Cold Acclimation in Arabidopsis. *Plant Physiol*
781 **171:** 2744-2759. DOI: https://doi.org/10.1104/pp.16.00533
782 **Zhao, Y, Zhu, P, Hepworth, J, Bloomer, R, Antoniou-Kourounioti, RL, Doughty, J,**
783 **Heckmann, A, Xu, C, Yang, H, Dean, C.** 2021. Natural temperature fluctuations
784 promote COOLAIR regulation of FLC. *Genes Dev* **35:** 888-898. DOI:
785 https://doi.org/10.1101/gad.348362.121

Figure legends

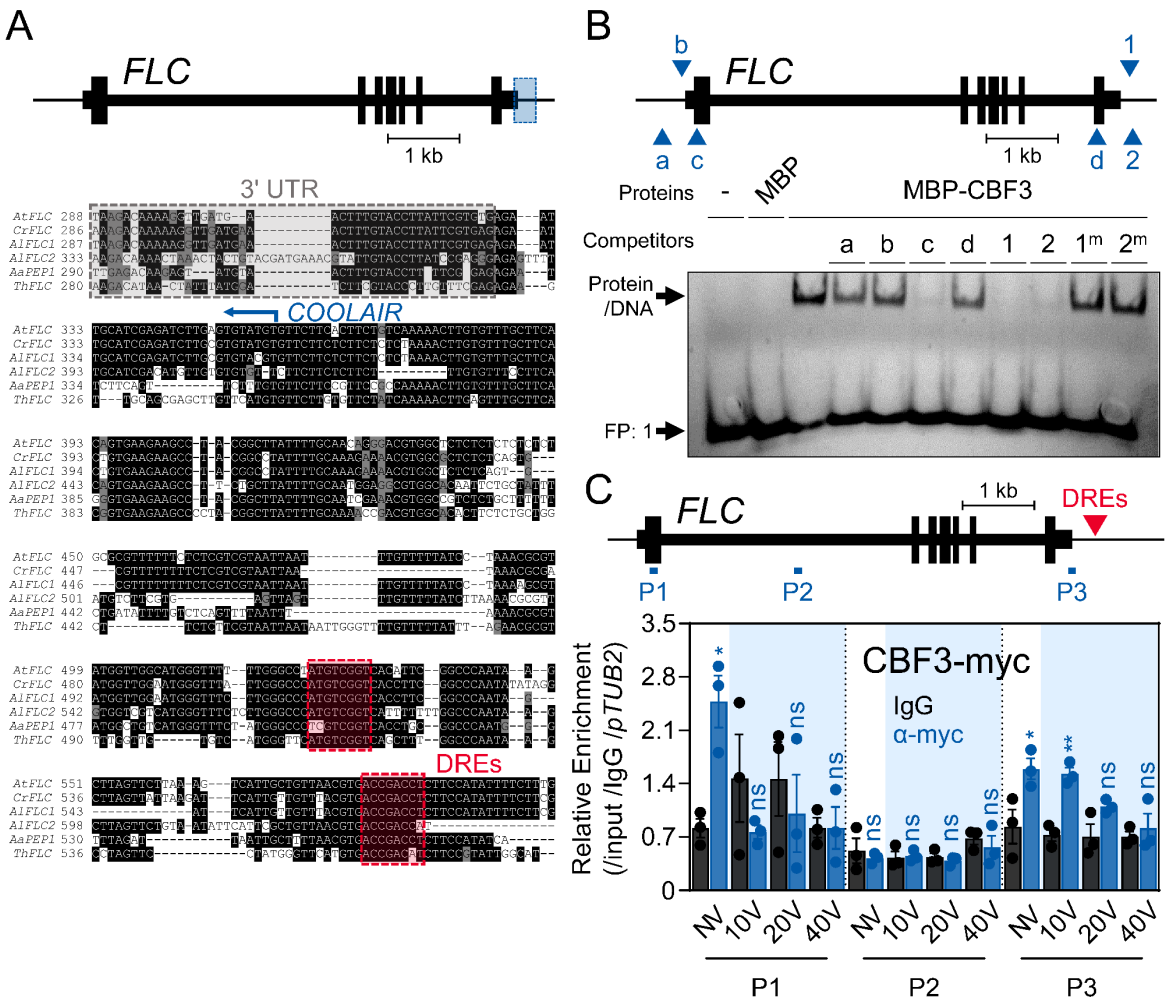

Figure 1. CBF3 directly binds to the CRT/DREs at the 3′-end of *FLC*.

(A) Comparison of sequences around the 3′-end of the *FLC* orthologs from Arabidopsis relatives. The upper graphic presents the gene structure of *AtFLC*. The black bars, thick lines, thicker lines indicate exons, introns, and UTRs, respectively. The blue-coloured box presents the region used for sequence comparison among 6 orthologous genes from 5 plant species. In the sequence alignment below, the grey box indicates the 3′-UTR of *FLC* orthologs, the blue arrow indicates the transcriptional start site of *AtCOOLAIR*, and the red dotted boxes indicate CRT/DREs. At, *Arabidopsis thaliana*; Cr, *Capsella rubella*; Al, *Arabidopsis lyrata*; Aa, *Arabis*

796 *alpina*; Th, *Thellungiella halophila*.

797 (B) EMSA using one of the CRT/DREs located at the *COOLAIR* promoter, DRE1, as a probe.
798 In the upper graphic showing *AtFLC* gene structure, CRT/DRE-like sequences are marked as
799 blue arrows and labelled as a, b, c, d for CRT/DRE-like sequences and as 1, 2 for CRT/DRE
800 sequences. For the competition assay, these CRT/DRE-like sequences and mutant forms of
801 DRE1, DRE2 were used as competitors. A 100-fold molar excess of unlabelled competitors
802 was added. FP, free probe.

803 (C) ChIP assay result showing the enrichment of CBF3-myc protein on the *AtFLC* locus.
804 Samples of NV, 10V, 20V, and 40V plants of *pSuper::CBF3-myc* were collected at zeitgeber
805 time (ZT) 4 in an SD cycle. The CBF3-chromatin complex was immunoprecipitated (IP) with
806 anti-myc antibodies (blue bars), and mouse IgG (black bars) was used as a control. Positions
807 of qPCR amplicons used for ChIP-qPCR analysis are illustrated as P1, P2, and P3 in the upper
808 graphic. The red arrow in the graphic denotes the position of two CRT/DREs located on the
809 *COOLAIR* promoter. ChIP-qPCR results have been represented as mean ± SEM of the 3
810 biological replicates in the lower panel. Dots represent each data-point. Relative enrichments
811 of the IP/5% input were normalized to that of *pTUB2*. The blue shading indicates a cold period.
812 Asterisks indicate a significant difference between IgG and anti-myc ChIP-qPCR results at
813 each vernalization time-point (*, $P<0.05$; **, $P<0.01$; unpaired Student's *t*-test). ns, not
814 significant.

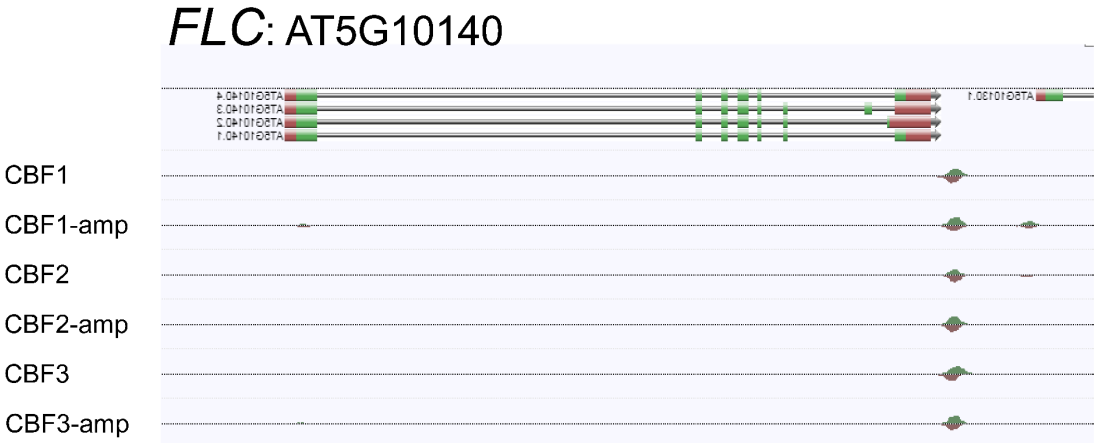

Figure 1—figure supplement 1. CBF proteins directly bind to the sequence at the 3′-end of *FLC* in DNA affinity purification sequencing (DAP-seq).

DAP-seq results showed enrichment of CBF proteins at the *AtFLC* locus obtained from the Plant Cistrome Database (http://neomorph.salk.edu/dev/pages/shhuang/dap_web/pages/index.php; *O'Malley et al., 2016*). The top bars represent the structures of alternatively spliced forms of the *FLC* transcript. The green, grey, and red bars indicate the exons, introns, and UTRs of *FLC*, respectively. The peaks below represent the positions of the CBF enrichments. CBF-amp; Amplification of DAP-seq results.

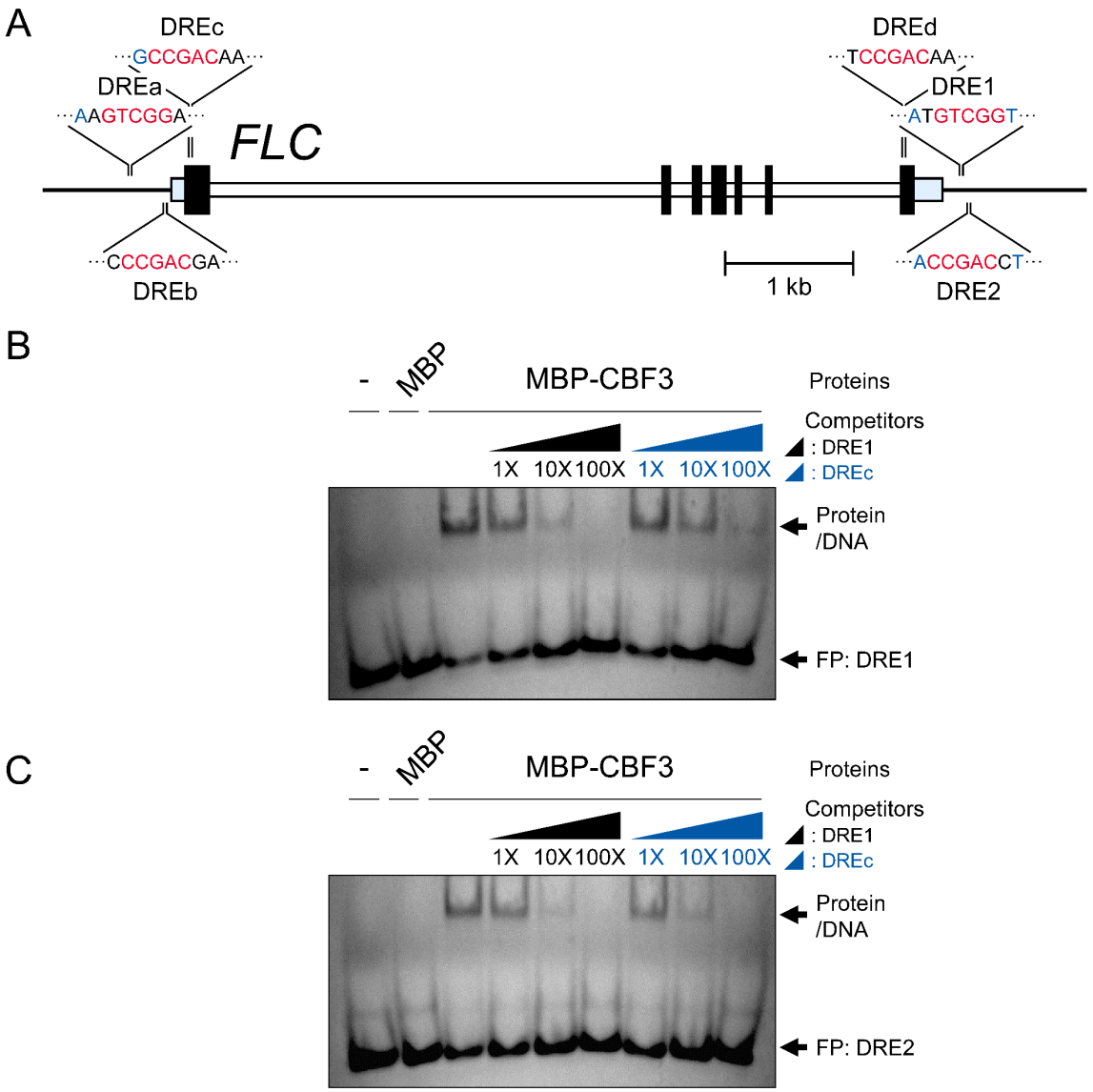

Figure 1—figure supplement 2. CBF3 binds to DRE1 and DRE2 on the *COOLAIR* promoter and DREc on the first exon of *FLC*.

(A) Schematic showing the positions of six CRT/DRE-like sequences distributed on the *AtFLC* locus. CRT/DRE sequences have been labelled as DRE1, -2, and CRT/DRE-like sequences have been labelled as DREa, -b, -c, and -d. The black bars, white lines, and light blue lines represent exons, introns, and UTRs of *AtFLC*, respectively. The red-coloured bases indicate the core sequence (CCGAC) of CRT/DRE. The blue-coloured bases represent bases known to

832 determine the binding affinity of CBF3 to CRT/DRE (*Maruyama et al., 2004*).

833 (B-C) EMSA using DRE1 (B) or DRE2 (C) as probe. For competition assay, DRE1, DRE2,
834 and DREc were used as competitors. Molar excess (1-, 10-, and 100-fold) of unlabelled
835 competitors was added. FP, free probe.

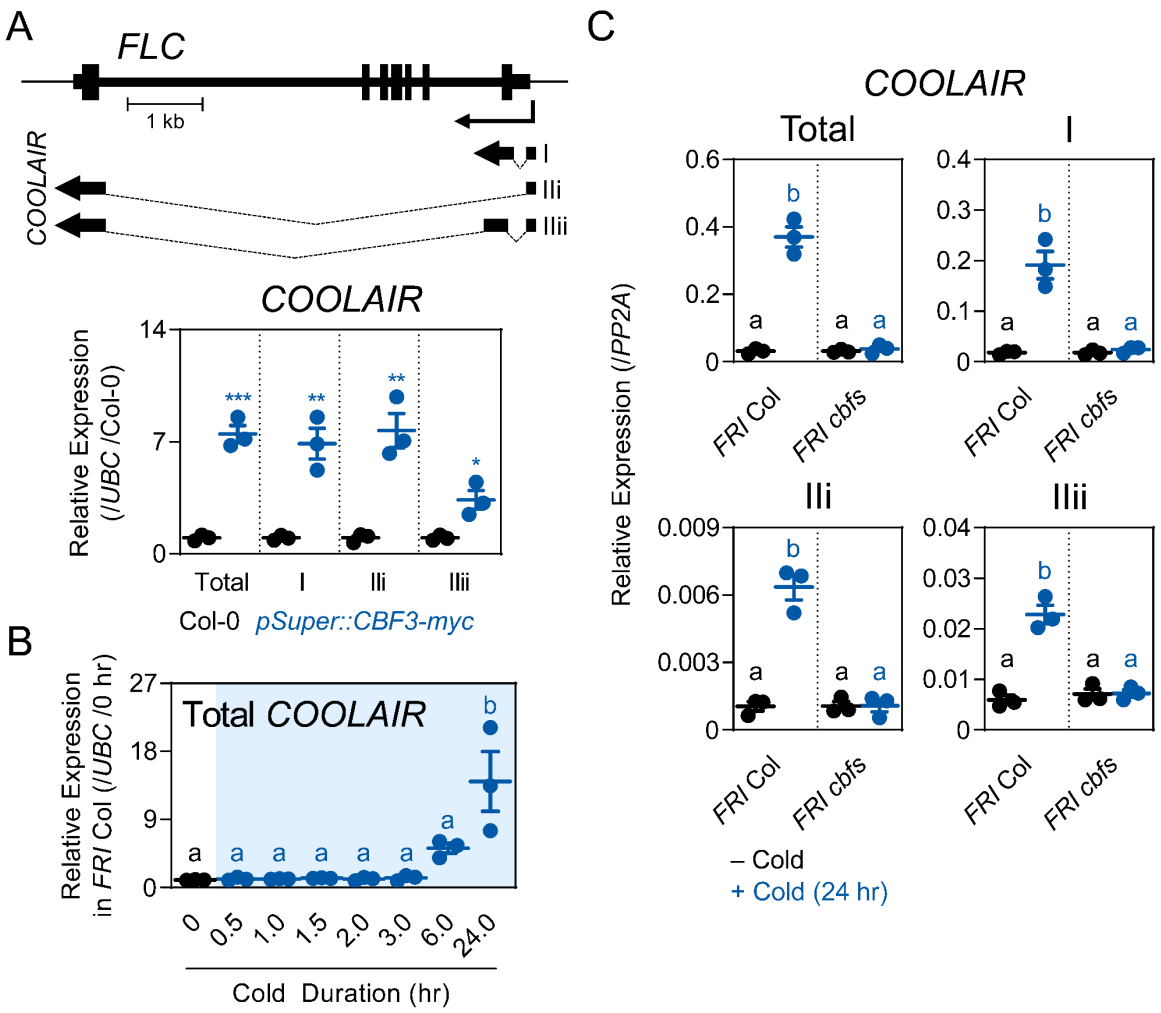

Figure 2. *COOLAIR* is one of the CBF regulons.

(A) Expression levels of total *COOLAIR* and *COOLAIR* isoforms in the wild-type (Col-0) and *CBF3*-overexpressing plants (*pSuper::CBF3-myc*). The gene structures of *FLC* and *COOLAIR* variants are illustrated in the upper panel. The thin black arrow indicates the transcriptional start site of *COOLAIR*. The thick black arrows indicate exons of each *COOLAIR* isoform. The structures of proximal (I) and distal (IIi and IIiii) *COOLAIR* isoforms are shown. The primer sets used for total, proximal (I), and distal (IIi, IIiii) COOLAIRs are marked in Figure 2-supplement 1. Relative transcript levels of total *COOLAIR* and *COOLAIR* variants have been represented as mean ± SEM of 3 biological replicates. Relative expression levels of *UBC* were

846 normalized to that of Col-0. Dots represent each data-point. Asterisks indicate a significant
847 difference, as compared to the wild-type (*, $P<0.05$; **, $P<0.01$; ***, $P<0.001$; unpaired
848 Student's *t*-test).

849 (B) Expression dynamics of total *COOLAIR* after short-term cold (0, 0.5, 1, 1.5, 2, 3, 6, and 24
850 h) treatment. Wild-types (*FRI* Col) were subjected to 4°C cold and harvested at each time-point.
851 Relative transcript levels of total *COOLAIR* to *UBC* were normalized to that of non-cold-
852 treated wild-type. The values have been represented as mean ± SEM of 3 biological replicates.
853 Dots represent each data-point. The blue shading indicates periods under cold treatment.
854 Significant differences have been marked using different letters (a, b; $P<0.05$; one-way
855 ANOVA followed by Tukey's post-hoc test).

856 (C) Transcript levels of total *COOLAIR* and *COOLAIR* isoforms in wild-type and *cbfs-1* mutant
857 before (–Cold) and after (+Cold) a day of 4°C cold treatment. Relative levels of total *COOLAIR*
858 and *COOLAIR* variants were normalized to that of *PP2A*. Values have been represented as
859 mean ± SEM of 3 biological replicates. Dots indicate each data-point. Significant differences
860 have been marked using different letters (a, b; $P<0.05$; two-way ANOVA followed by Tukey's
861 post-hoc test).

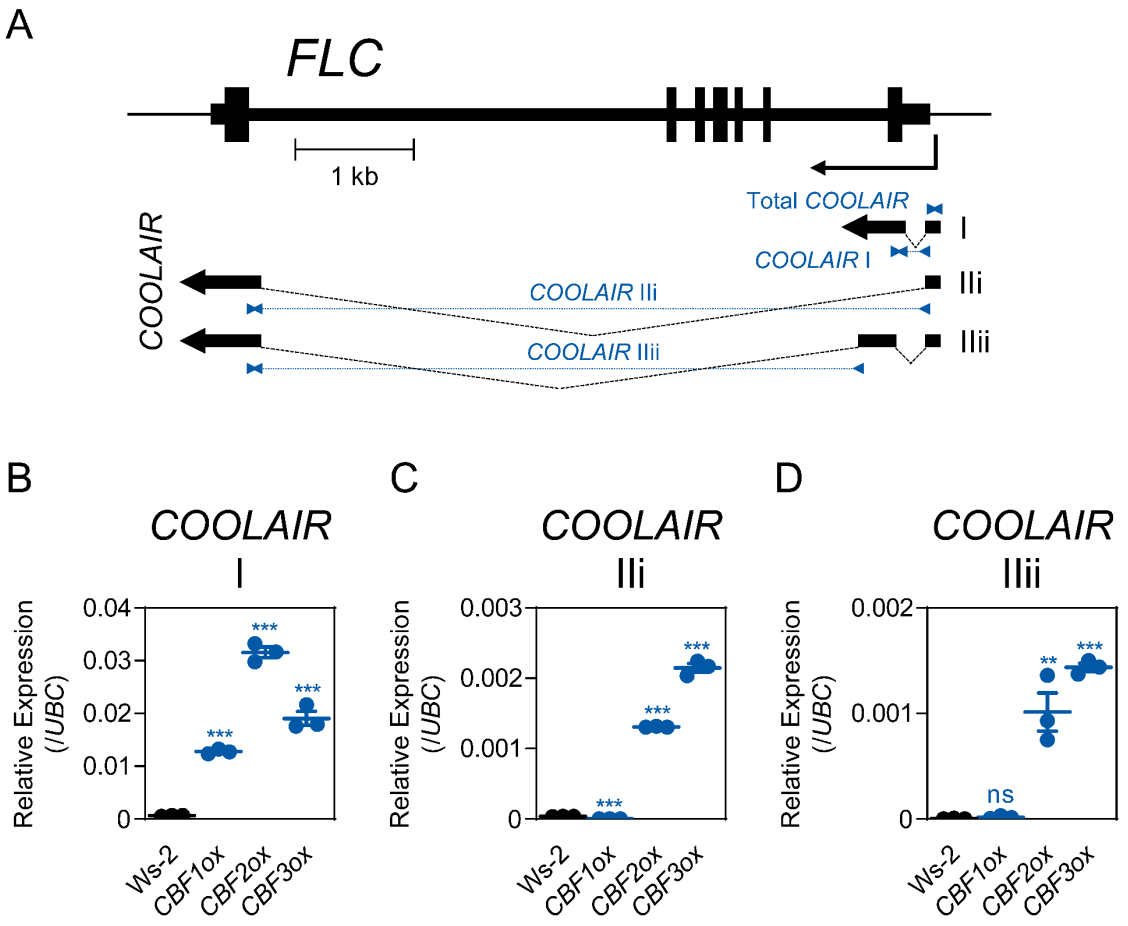

863 **Figure 2—figure supplement 1. Overexpression of *CBF1*, *-2*, or *-3* causes an increase in**
864 ***COOLAIR* level, but the effects on *COOLAIR* variants are subtly different.**

865 (A) Positions of qPCR amplicons used for detecting proximal (I) and distal (IIi and IIIi)
866 *COOLAIR* variants. The black bars denote exons, thin lines denote introns, and thick lines
867 denote UTRs of *FLC*. The thin black arrow below the gene structure indicates the
868 transcriptional start site of *COOLAIR*. The thick black arrows below denote exons of the type
869 I, type IIi, and type IIIi *COOLAIR* variants. The positions of qPCR amplicons used for the
870 qPCR analysis have been marked using blue arrows.

871 (B-D) Transcript levels of *COOLAIR* variants in the wild-type (Ws-2) and *CBF1-*, *-2-*, and *-3-*
872 overexpressing transgenic plants (*CBF1ox*, *CBF2ox*, and *CBF3ox*, respectively*; Seo et al.,*
873 *2009*). Relative levels of type I (B), type IIi (C), and type IIIi (D) *COOLAIR* were normalized

874 to that of *UBC*. Values have been represented as mean ± SEM of 3 biological replicates. Dots
875 represent each data-point. Asterisks indicate a significant difference, as compared to the wild-
876 type (**, $P<0.01$; ***, $P<0.001$; unpaired Student's *t*-test). ns, not significant.

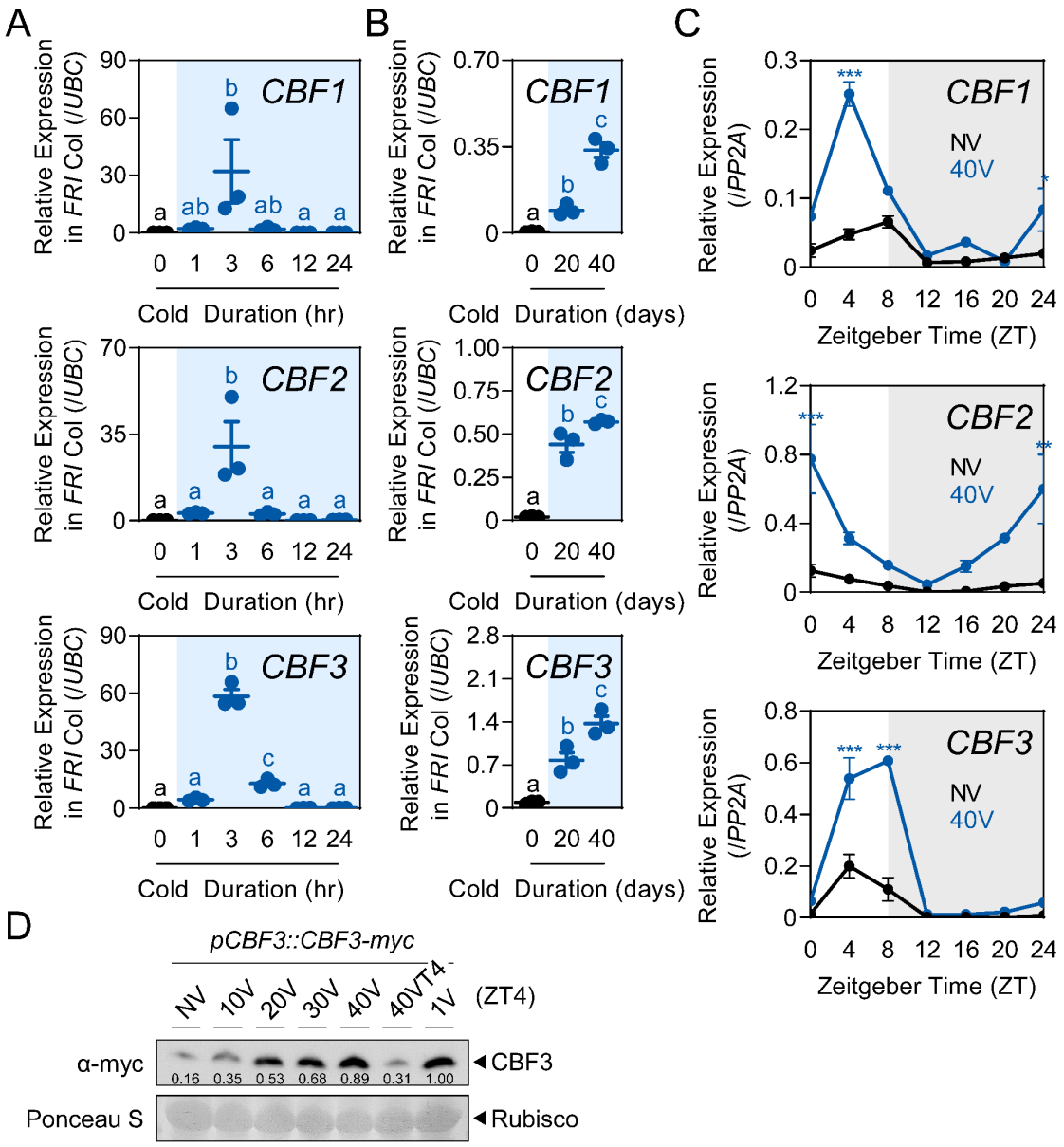

878 **Figure 3. Protein levels of CBFs increase during the vernalization process.**

879 (A) Transcript levels of *CBF1*, *-2*, and *-3* under short-term cold exposure. Wild-type plants
880 were subjected to 0, 1, 3, 6, 12, and 24 h of 4°C cold treatment. Relative levels of *CBF1*, *-2*,
881 and *-3* were normalized to that of *UBC*. Values have been represented as mean ± SEM of 3
882 biological replicates. Dots represent each data-point. The blue shadings indicate periods under
883 cold period. Significant differences have been marked using different letters (a-c; $P<0.05$; one-

884 way ANOVA followed by Tukey's post-hoc test).

885 (B) Transcript levels of *CBF1*, *-2*, and *-3* after 20V and 40V. Wild-type plants were treated with
886 4°C vernalization under an SD cycle and collected at ZT4. Relative levels of *CBF1*, *-2*, and *-3*
887 were normalized to that of *UBC*. Values have been represented as mean ± SEM of 3 biological
888 replicates. Dots indicate each data-point. The blue shadings denote periods under cold period.
889 Significant differences have been marked using different letters (a-c; $P<0.05$; one-way ANOVA
890 followed by Tukey's post-hoc test).

891 (C) Daily rhythms of *CBF1*, *-2*, and *-3* transcript levels in NV or 40V plants. Col-0 plants
892 grown under an SD cycle were collected every 4 h between ZT0 and ZT24. Relative transcript
893 levels of *CBF1*, *-2*, and *-3* were normalized to that of *PP2A*. Values have been represented as
894 mean ± SEM of 3 biological replicates. The grey shadings represent dark periods. Asterisks
895 indicate a significant difference between NV and 40V at each time-point (*, $P<0.05$; **, $P<0.01$;
896 ***, $P<0.001$; two-way ANOVA followed by Tukey's post-hoc test).

897 (D) Increase of CBF3 protein level during the vernalization process. The *pCBF3::CBF3-myc*
898 transgenic plants, subjected to 4°C vernalization, were collected at ZT4 of the indicated time-
899 point. CBF3 proteins were detected using anti-myc antibodies. Rubisco was considered the
900 loading control. Numbers below each band indicate relative signal intensity compared to 1V.
901 The mean values of 3 biological replicates are presented.

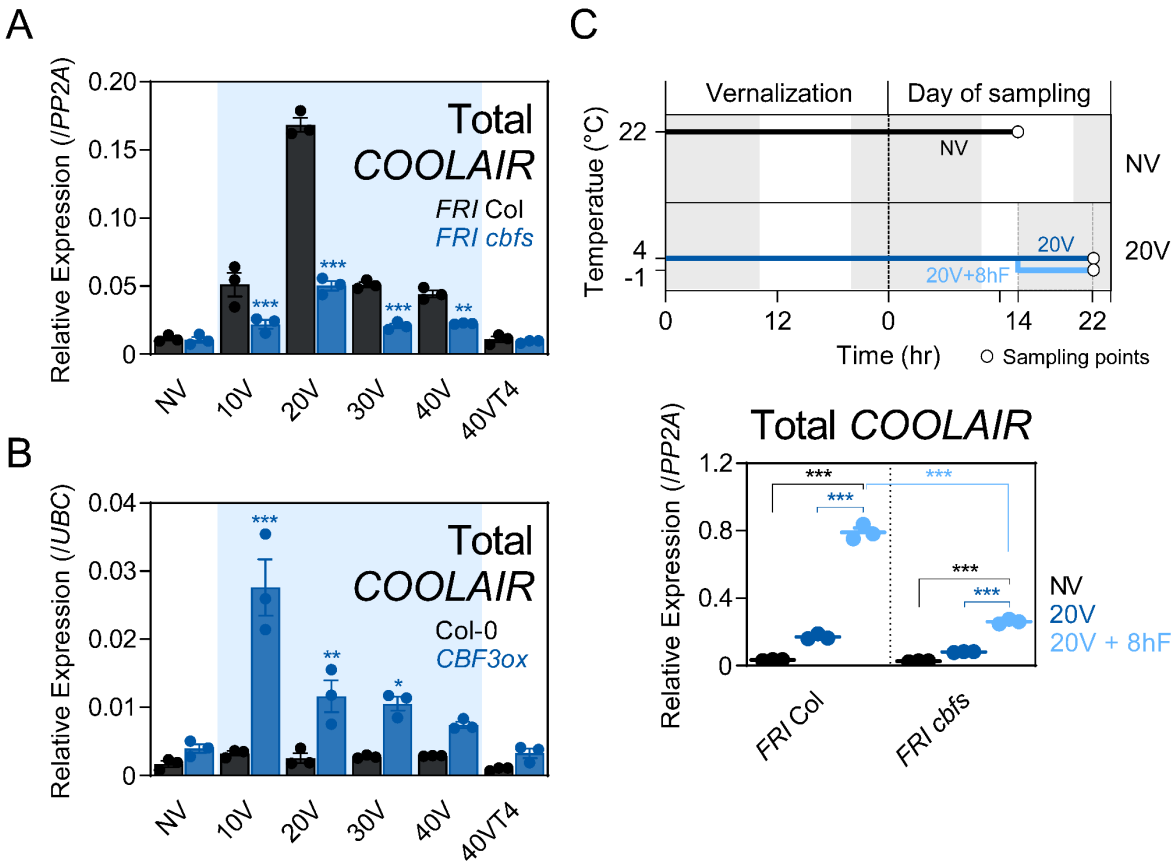

Figure 4. *CBF*s are involved in vernalization-induced *COOLAIR* expression.

(A) Expression dynamics of total *COOLAIR* in wild type and *cbfs-1* mutant during vernalization. Relative transcript levels of total *COOLAIR* were normalized to that of *PP2A*. Values have been represented as mean ± SEM of 3 biological replicates. Dots represent each data-point. Asterisks indicate a significant difference between wild-type and *cbfs-1* mutant at each time-point (**, $P<0.01$; ***, $P<0.001$; two-way ANOVA followed by Tukey's post-hoc test).

(B) Transcript level of total *COOLAIR* in wild-type (Col-0) and CBF3-overexpressing transgenic plant (*CBF3ox; pSuper::CBF3-myc*) during vernalization. Relative levels of total *COOLAIR* were normalized to that of *PP2A*. Values have been represented as mean ± SEM of 3 biological replicates. Dots represent each data-point. Asterisks indicate a significant difference between the wild-type and *CBF3* overexpressor (*, $P<0.05$; **, $P<0.01$; ***,

915 *P*<0.001; two-way ANOVA followed by Tukey's post-hoc test). Blue shading denotes cold
916 periods in (A) and (B).

917 (C) Effect of first frost-mimicking treatment [8 h of freezing (<0°C)] on the level of total
918 *COOLAIR* in 20V wild-type and *cbfs-1*. The upper panel shows a schematic of the experimental
919 procedure. For NV, wild-type and *cbfs-1* were collected at ZT4 after growing at 22°C for 16 d.
920 For the first frost treatment, 20V wild-type and *cbfs-1* mutant were treated with an additional
921 8 h of 4°C (20V, blue line) or 8 h of -1°C (20V+8hF, light blue line) under dark, and then the
922 whole seedlings were collected at ZT22 for analysis. All the plants were grown under an SD
923 cycle. The grey shadings denote dark periods. Total *COOLAIR* levels in wild-type and *cbfs-1*
924 treated with NV, 20V, and 20V+8hF have been represented as mean ± SEM of 3 biological
925 replicates in the lower panel. Dots indicate each data-point. Relative levels of total *COOLAIR*
926 were normalized to that of *PP2A*. Asterisks indicate a significant difference (***, *P*<0.001;
927 two-way ANOVA followed by Tukey's post-hoc test).

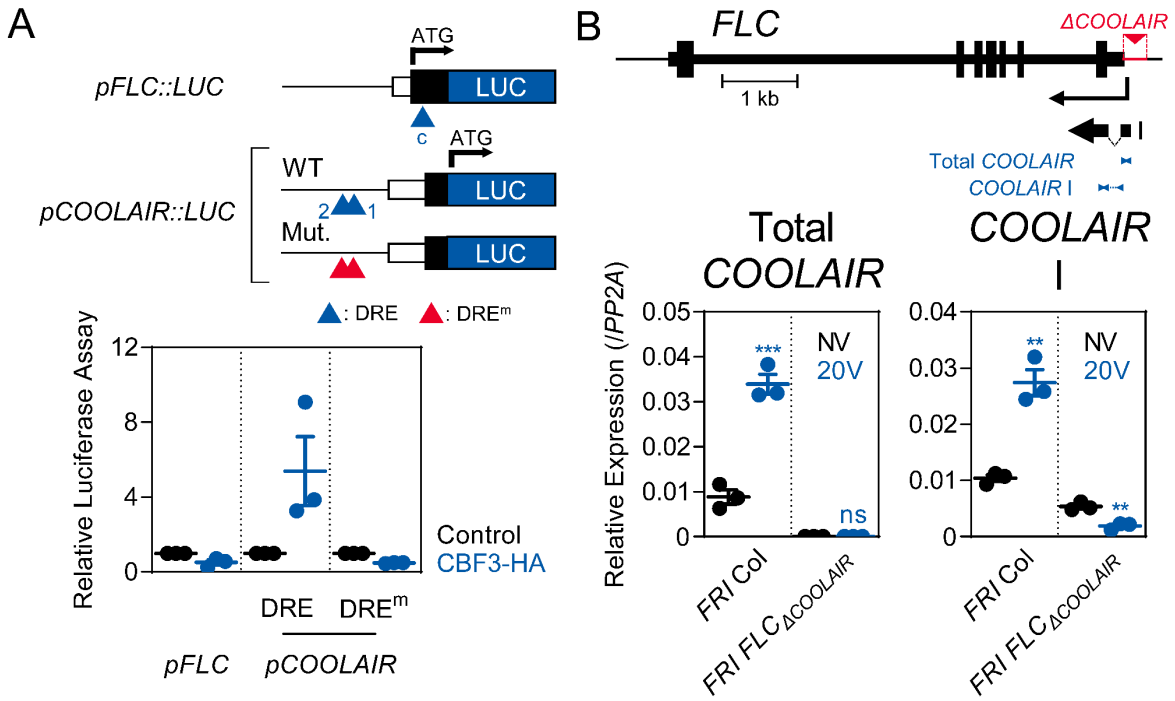

929 **Figure 5. *COOLAIR* promoter containing CRT/DREs is necessary for CBFs-mediated**
930 **vernalization induction.**

931 (A) Luciferase assay showing that CBF3 activates *COOLAIR* promoter with wild-type
932 CRT/DRE (DRE) but fails to activate the one with mutant CRT/DRE (DRE^m). A schematic of
933 the reporter constructs used for the luciferase assay is presented in the upper panel. *pFLC::LUC*
934 harbors 1 kb of the promoter, the 5′-UTR, and the first exon of *FLC*. The blue arrow in the
935 *pFLC::LUC* graphic indicates the location of DREc. Wild-type (WT) and mutant (Mut) forms
936 of *pCOOLAIR::LUC* include 1 kb of the *COOLAIR* promoter with the 3′-UTR and last exon of
937 *FLC*. The blue and red arrows mark the positions of the wild-type (DRE) and mutant (DRE^m)
938 forms of DRE1 and DRE2, respectively. Each reporter construct was co-transfected into *A.*
939 *thaliana* protoplast together with the *35S::CBF3-HA* effector construct. In parallel, *35S-NOS*
940 control plasmid was transfected as a control. The result is shown below. Relative luciferase
941 activities were normalized to that of the *35S-NOS* control. Values have been represented as
942 mean ± SEM of 3 biological replicates. Dots represent each data-point.

943 (B) Transcript levels of total *COOLAIR* and proximal (I) *COOLAIR* isoform in wild-type and

944 *FLC*$_{\Delta COOLAIR}$ mutant before (NV) and after vernalization (20V). *FLC*$_{\Delta COOLAIR}$ has a 324 bp
945 deletion of the *COOLAIR* promoter region containing DRE1 and -2 (*Luo et al., 2019*). The
946 position of the deleted region is marked in red lines with reversed triangle in the upper graphic.
947 Black bars denote exons, thin lines denote introns, and thick lines denote UTRs of *FLC*. The
948 thin black arrow below the gene structure indicates the transcriptional start site of *COOLAIR*.
949 The thick black arrow below denotes exons of the type I *COOLAIR* variant. The positions of
950 amplicons used for the qPCR analysis are marked as blue arrows. The qPCR analysis result is
951 presented in the lower panel. Relative transcript levels were normalized to that of *PP2A*. Values
952 have been represented as mean ± SEM of 3 biological replicates. Dots represent each data-
953 point. Asterisks indicate a significant difference, as compared to NV (**, $P<0.01$; ***, $P<0.001$;
954 unpaired Student's *t*-test). ns, not significant.

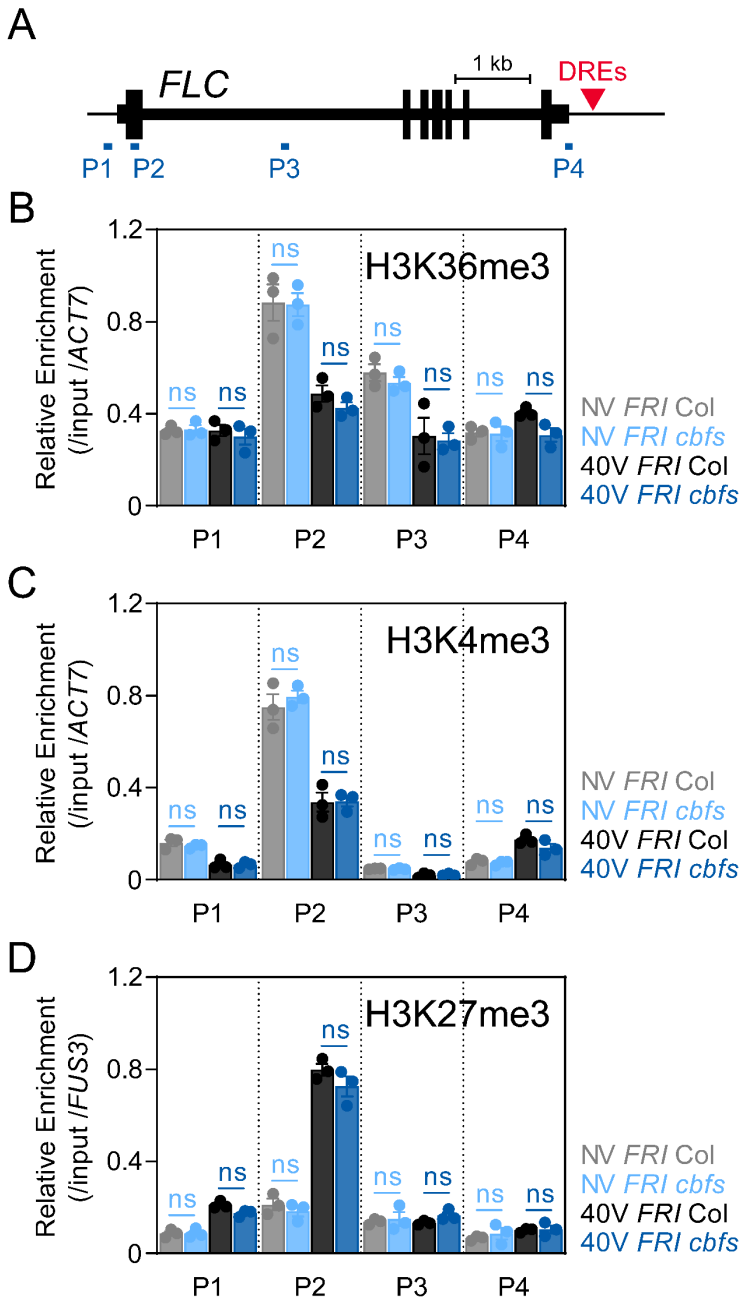

956 **Figure 6. Histone modifications on *FLC* chromatin are not affected by *cbfs* mutation.**

957 (A) Schematic representation of *FLC* gene structure showing the positions of qPCR amplicons
958 used for ChIP analysis. The red arrow presents the position of two CRT/DREs in the *COOLAIR*
959 promoter. qPCR amplicons are marked as blue bars labelled P1, P2, P3, and P4.

960 (B-D) Enrichments of H3K36me3 (B), H3K4me3 (C), and H3K27me3 (D) on the *FLC* locus
961 in NV or 40V wild-type and *cbfs-1* plants. The whole seedlings were collected at ZT4 under an
962 SD cycle. Modified histones were immunoprecipitated with anti-H3K36me3, anti-H3K4me3,
963 or anti-H3K27me3 antibodies. H3K36me3, H3K4me3, and H3K27me3 enrichments of the
964 IP/5% input at P1, P2, P3, and P4 were normalized to those of *ACT7* and *FUS3*. Relative
965 enrichments have been represented as mean ± SEM of 3 biological replicates. Dots represent
966 each data-point. ns, not significant between wild-type and *cbfs-1*, as assessed using two-way
967 ANOVA followed by Tukey's post-hoc test (P>0.05).

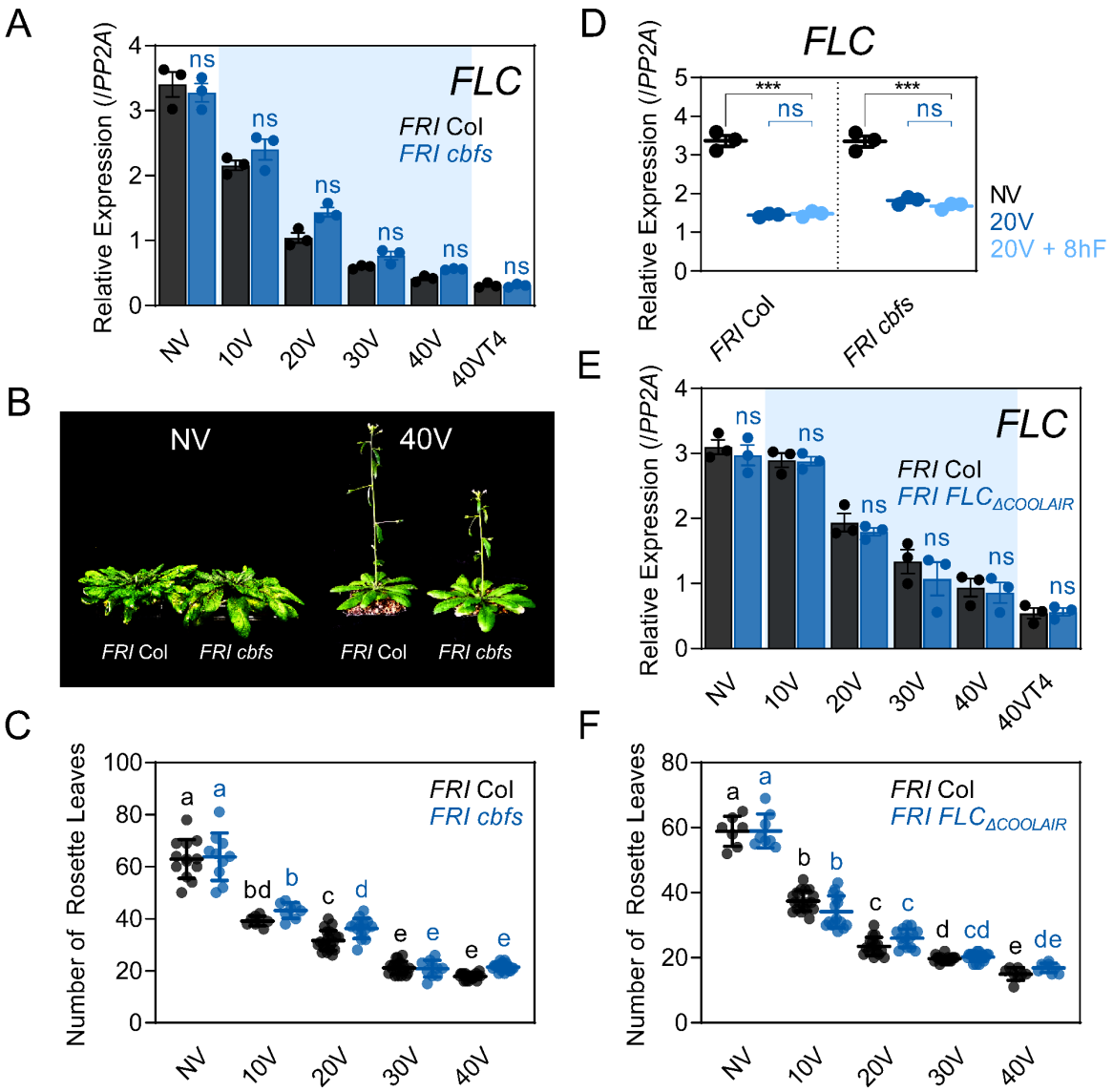

Figure 7. *CBF*-mediated *COOLAIR* induction under long-term cold is not absolutely necessary for *FLC* silencing.

(A) Transcript levels of *FLC* mRNA in wild-type and *cbfs-1* during vernalization. Blue shading denotes cold periods. Relative levels were normalized to that of *PP2A*. Values have been represented as mean ± SEM of 3 biological replicates. Dots represent each data-point. ns, not significant between wild-type and *cbfs-1*, as assessed using two-way ANOVA followed by Tukey's post-hoc test (P>0.05).

976 (B) Photographs of NV and 40V wild-type and *cbfs-1*. NV plants were grown at 22°C under
977 LD and 40V plants were grown at 22°C under LD after being treated for 40V under SD. The
978 photos were taken when the NV plants started to bolt and the 40V plants showed the first open
979 flower.

980 (C) Flowering times of NV and vernalized (10V-40V) wild-type and *cbfs-1* plants. Flowering
981 time was measured in terms of the number of rosette leaves produced when bolting. Plants
982 were grown under LD after vernalization treatment. Bars and error bars represent the mean ±
983 standard deviation (SD) of 3 biological replicates. Each dot indicates individual flowering time.
984 Significant differences have been marked using different letters (a-e; two-way ANOVA
985 followed by Tukey's post-hoc test; $P<0.05$).

986 (D) Effect of the first frost-mimicking treatment (8 h freezing) on *FLC* mRNA level in wild-
987 type and $FLC_{\Delta COOLAIR}$ after 20V. NV, 20V, and 20V+8hF plants were subjected to the treatments
988 described in *Figure 4C*. Relative levels were normalized to that of *PP2A*. Values have been
989 represented as mean ± SEM of 3 biological replicates. Dots represent each data-point. Asterisks
990 indicate a significant difference (***$P<0.001$; two-way ANOVA followed by Tukey's post-hoc
991 test). ns, not significant.

992 (E) Transcript levels of *FLC* mRNA in wild-type and *cbfs-1* during vernalization. Blue shading
993 denotes cold periods. Bars and error bars represent mean ± SEM of 3 biological replicates. Dots
994 represent each data-point. ns, not significant between wild-type and $FLC_{\Delta COOLAIR}$, as assessed
995 using two-way ANOVA followed by Tukey's post-hoc test ($P>0.05$).

996 (F) Flowering times of non-vernalized (NV) and vernalized (10V-40V) wild-type and
997 $FLC_{\Delta COOLAIR}$. Flowering time was measured in terms of the number of rosette leaves produced
998 when bolting. Plants were grown under LD after vernalization. Bars and error bars indicate
999 mean ± SD. Each dot represents individual flowering time. Significant differences have been
1000 indicated using different letters (a-e; two-way ANOVA followed by Tukey's post-hoc test;
1001 $P<0.05$).

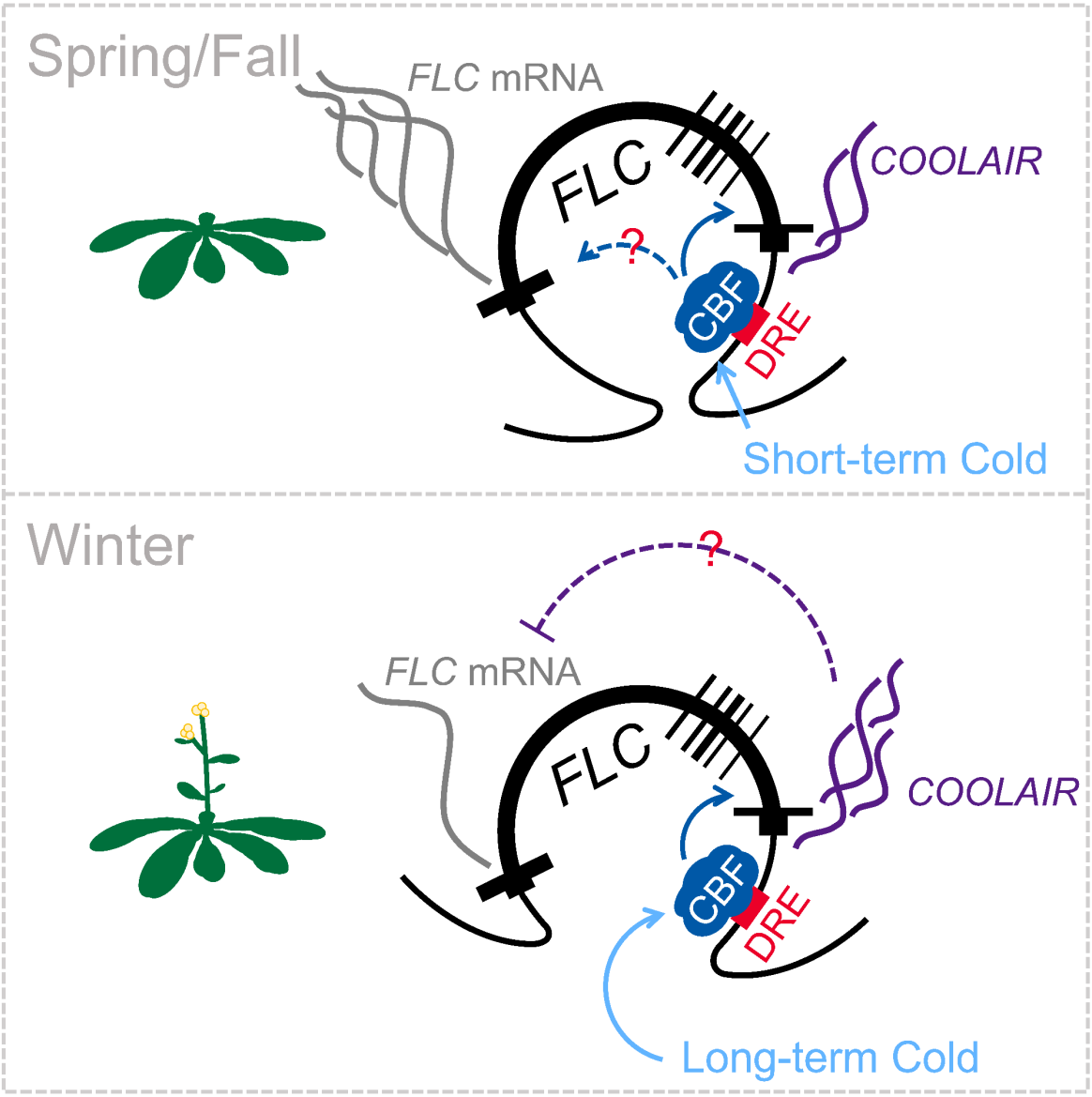

1003 **Figure 8. Schematic model describing the mechanism of CBFs-mediated *COOLAIR***
1004 **expression during the early phase of vernalization.**

1005 During the early phase of vernalization, increased CBF upregulates *COOLAIR* expression by
1006 binding to the CRT/DREs at the 3′-end of *FLC*. In the late phase of vernalization, CBF proteins
1007 fall off from CRT/DREs in the *COOLAIR* promoter, which leads to a reduction in *COOLAIR*
1008 levels.